

Fast and Adaptive Multi-agent Planning under Collaborative Temporal Logic Tasks via Poset Products

Zesen Liu¹, Meng Guo¹, Weimin Bao² and Zhongkui Li¹

Abstract—Efficient coordination and planning is essential for large-scale multi-agent systems that collaborate in a shared dynamic environment. Heuristic search methods or learning-based approaches often lack the guarantee on correctness and performance. Moreover, when the collaborative tasks contain both spatial and temporal requirements, e.g., as Linear Temporal Logic (LTL) formulas, formal methods provide a verifiable framework for task planning. However, since the planning complexity grows exponentially with the number of agents and the length of the task formula, existing studies are mostly limited to small artificial cases. To address this issue, a new planning paradigm is proposed in this work for system-wide temporal task formulas that are released online and continually. It avoids two common bottlenecks in the traditional methods, i.e., (i) the direct translation of the complete task formula to the associated Büchi automaton; and (ii) the synchronized product between the Büchi automaton and the transition models of all agents. Instead, an adaptive planning algorithm is proposed that computes the product of relaxed partially-ordered sets (R-posets) on-the-fly, and assigns these subtasks to the agents subject to the ordering constraints. It is shown that the first valid plan can be derived with a polynomial time and memory complexity w.r.t. the system size and the formula length. Our method can take into account task formulas with a length of more than 400 and a fleet with more than 400 agents, while most existing methods fail at the formula length of 25 within a reasonable duration. The proposed method is validated on large fleets of service robots in both simulation and hardware experiments.

I. INTRODUCTION

Recent advances in computation, perception and communication allow the deployment of autonomous robots in large, remote and hazardous environments, e.g., to assist service staff in hospitals [1], to maintain offshore drilling platforms [2], to monitor and assist construction sites [3]. Furthermore, fleets of heterogeneous robots, such as unmanned ground vehicles and unmanned aerial vehicles, are deployed to accomplish tasks that are otherwise too inefficient or even infeasible for a single robot [4]. Not only the overall efficiency of the team can be significantly improved by allowing the robots to move and act concurrently [5]; but also the capabilities of the team can be greatly extended by enabling multiple robots to directly collaborate on a task [6]. Recent works have

¹The authors are with the State Key Laboratory for Turbulence and Complex Systems, Department of Mechanics and Engineering Science, College of Engineering, Peking University, Beijing 100871, China. E-mail: 1901111653, meng.guo, zhongkui.li@pku.edu.cn

²The author is with Science and Technology Commission of China Aerospace Science and Technology Corporation, Beijing 100048, China. E-mail:BAOWEIMIN@CASHQ.AC.CN

demonstrated such potentials preliminary for simple tasks such as collaborative exploration [7], formation control [8], object transportation [9] and pursuer-evader games [10]. The task planning problem for multi-robot systems is in general NP-hard [11], due to the inherent combinatorial nature of robot-task assignment and various constraints such as capabilities and deadlines. The standard approach is to formulate a mixed integer linear programs (MILP) over the integer variables and constraints [12]. Whereas being sound and optimal, these methods are applicable to only small-scale systems. Thus, extensive work can be found on designing meta-heuristic algorithms for finding sufficiently good solutions in a reasonable time, e.g., genetic algorithms [13], colony optimization [14], [15], particle swarm optimization [16], [17], learning-based algorithms [18], [19], [20], or large language models [21], [22]. However, these methods often lack a formal guarantee on the correctness and quality of the planning results.

Moreover, to specify more complex tasks, many recent works propose to use formal languages such as Linear Temporal Logic (LTL) [23], Computation Tree Logic (CTL) [24], and Signal Temporal Logic (STL) [25], as an intuitive yet powerful way to describe both spatial and temporal requirements on global [26] or local [27] behaviors. Notably, the works in [28], [29], [30] formulate MILP by a central planning unit given different system models and task constraints; the works in [31], [32], [33], [34], [35] instead propose various search algorithms over the state or solution space of the whole system. However, the aforementioned planning methods are often executed offline for a set of predefined static tasks. A particularly challenging scenario is when the system operates indefinitely, i.e., new tasks are released or canceled *dynamically* and *continually* by external demand [36]; or certain target features related to the tasks can change location during run time [10]. This would require the fleet to adaptively change their task plans online to modify existing assignments and incorporate new tasks. Thus, the aforementioned methods become inadequate as the sequence of tasks is infinite and their specifications are unknown beforehand. Recursive application of the centralized methods in a naive way leads to not only intractable computation complexity, but also inconsistent or even oscillatory assignments. Thus, an efficient and adaptive planning scheme is essential for multi-robot systems that collaborate in a dynamic environment [37], [38], [39] or an unknown environment [40].

A. Related Work

The standard framework for planning under temporal tasks is based on the model-checking algorithm [23]: First, the task formulas are converted to a Deterministic Robin Automaton (DRA) or Nondeterministic Büchi Automaton (NBA), via off-the-shelf tools such as SPIN [41] and LTL2BA [42]. Second, a product automaton is created between the automaton of formula and the models of all agents, such as weighted finite transition systems (wFTS) [23], Markov decision processes [43] or Petri nets [44]. Last, certain graph search or optimization procedures are applied to find a valid and accepting plan within the product automaton, such as nested-Dijkstra search [32], integer programs [45], auction [46] or sampling-based [33], [47].

Thus, the fundamental step of all aforementioned methods is to translate the task formula into the associated automaton. This translation may lead a double-exponential size w.r.t. the formula length as shown in [42]. The only exceptions are GR(1) formulas [48], of which the associated automaton can be derived in polynomial time but only for limited cases. In fact, for general LTL formulas with length more than 25, it takes more than 2 hours and 13GB memory to compute the associated NBA via LTL2BA. Although recent methods have greatly reduced the planning complexity in other aspects, the length of considered task specifications remains limited due to this translation process. For instance, the sampling-based method [33], [47] avoids creating the complete product automaton via RRT sampling, of which the largest simulated case has 400 agents and the task formula has a maximum length of 14. The planning method [32] decomposes the resulting task automaton into independent sub-tasks for parallel execution. The simulated case scales up to 100 robots and a task formula of maximum length 18. Moreover, other existing works such as [49], [50], [51], [52] mostly consider task formulas of length around 6-10. This limitation hinders its application to more complex robotic missions.

This drawback becomes even more apparent for dynamic scenes, where contingent tasks specified as LTL formulas are triggered by external observations and released to the whole team online. In such cases, most existing approaches compute the automaton associated with the new task, of which the synchronized product with the current automaton is derived, see e.g., [51], [52]. Thus, the size of the resulting automaton equals to the product of *all* automata associated with the contingent tasks, which is clearly a combinatorial blow-up. Consequently, the amount of contingent tasks that can be handled by the aforementioned approaches is limited to hand-picked examples.

B. Our Contribution

To overcome this curse of dimensionality in the size of tasks and agents, we propose a new paradigm that is *fundamentally* different from the model-checking-based methods. First, for a syntactically co-safe LTL (sc-LTL) formula that is a conjunction of numerous sub-formulas, we calculate the R-posets of each sub-formula as a set of subtasks and their partial temporal

constraints. Then, an efficient algorithm is proposed to compute the product of R-posets associated with each sub-formula. The resulting product of R-posets is complete in the sense that it retains all subtasks from each R-poset along with their partial orderings and resolves potential conflicts. Given this product, a task assignment algorithm called the time-bound contract net (TBCN) is proposed to assign collaborative subtasks to the agents, subject to the partial ordering constraints. Last but not least, the same algorithm is applied online to dynamic scenes where contingent tasks are triggered and released by online observations. It is shown formally that the proposed method has a polynomial time and memory complexity to derive the first valid plan w.r.t. the system size and formula length. Extensive large-scale simulations and experiments are conducted for a hospital environment where service robots react to online requests such as collaborative transportation, cleaning and monitoring.

Main contribution of this work is three-fold: (i) a systematic method is proposed to tackle task formulas with length more than 400, which overcomes the limitation of existing translation tools that can only process formulas of length less than 25 in reasonable time; (ii) an efficient algorithm is proposed to decompose and integrate contingent tasks that are released online, which not only avoids a complete re-computation of the task automaton but also ensures a polynomial complexity to derive the first valid plan; (iii) the proposed task assignment algorithm is fully compatible with both static and dynamic scenarios with interactive objects.

C. Problem Statement

Consider a multi-agent system with heterogeneous capabilities, a series of sc-LTL task formulas that are released online, and a set of interactive objects in the dynamic environment. The objective is to generate a task plan for the system online such that these tasks are satisfied with high efficiency.

For instance as shown in Sec. II-C, a fleet of heterogeneous service robots is deployed in the hospital environment. Different tasks such as transportation of goods or patients, cleaning and maintenance are released online continuously. Many of such tasks contain numerous subtasks with ordering constraints that require direct collaboration of different robots. An efficient coordination algorithm is proposed such that these subtasks are assigned and fulfilled online in a timely manner.

II. RESULTS

In this section, we present the proposed solution briefly, where we first give a definition of task specification and introduce the core method of computing the R-poset product. Then, an efficient assignment algorithm is introduced under these posets with temporal and spatial constraints. The simulation and hardware experiment results are presented, against several strong baselines for different sizes of fleets and task complexities. Technical details and derivations can be found in the section of “Materials and Methods”.

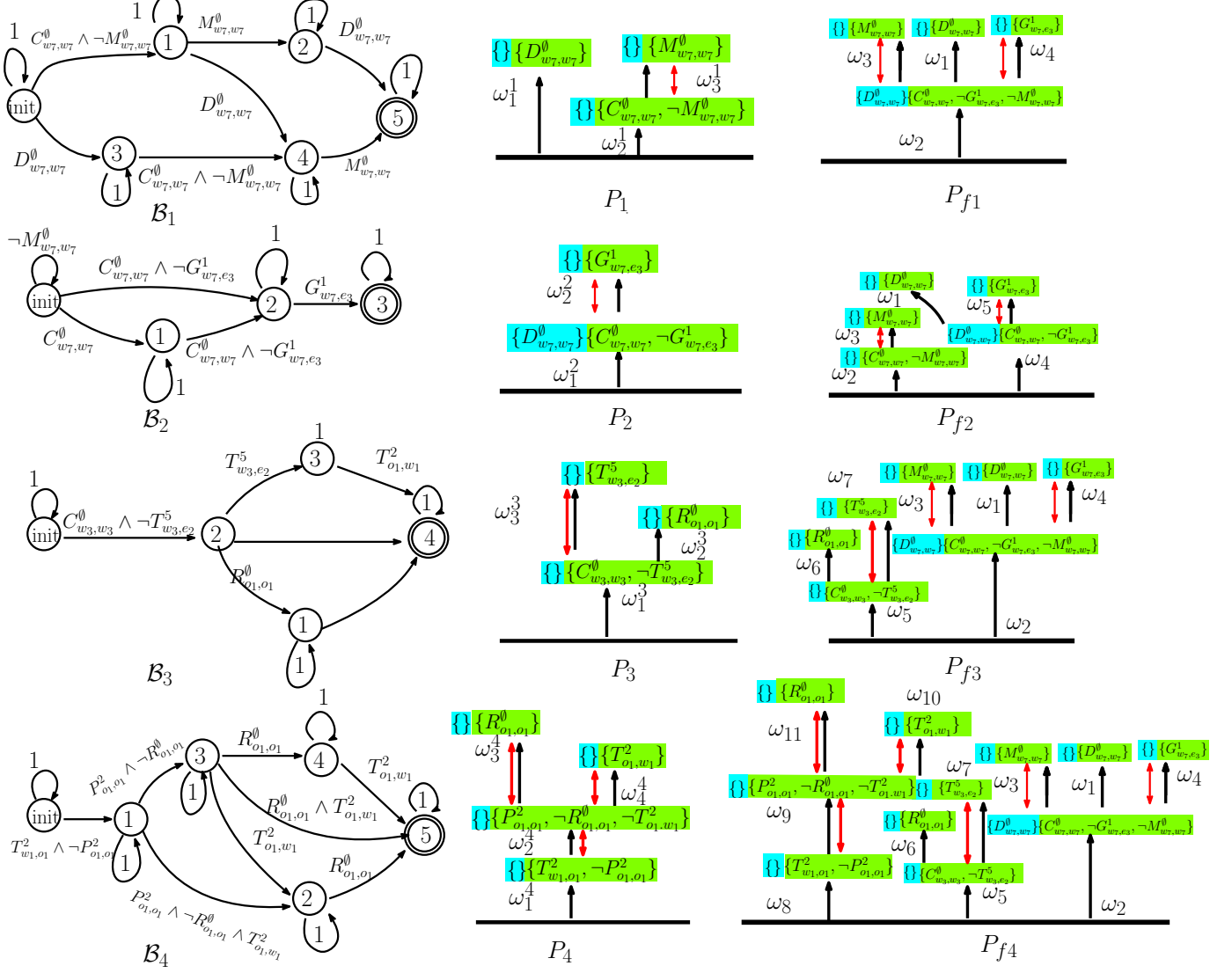


Fig. 1. Example of *Poset-Prod* associated with four formulas $\varphi_1 = \Diamond D_{w_7,w_7}^\emptyset \wedge \Diamond(C_{w_7,w_7}^\emptyset \wedge \neg M_{w_7,w_7}^\emptyset \wedge \Diamond M_{w_7,w_7}^\emptyset)$, $\varphi_2 = \Diamond(C_{w_7,w_7}^\emptyset \wedge \neg G_{w_7,e_3}^1 \wedge \Diamond G_{w_7,e_3}^1) \wedge \neg D_{w_7,w_7}^\emptyset \cup C_{w_7,w_7}^\emptyset$, $\varphi_3 = \Diamond(C_{w_3,w_3}^\emptyset \wedge \neg T_{w_3,e_2}^5 \wedge \Diamond D_{w_3,w_3}^\emptyset \wedge \Diamond T_{w_3,e_2}^5)$ and $\varphi_4 = \Diamond(T_{w_1,o_1}^2 \wedge \neg P_{o_1,o_1}^2 \wedge \Diamond(P_{o_1,o_1}^2 \wedge \neg R_{o_1,o_1}^\emptyset \wedge \Diamond T_{o_1,w_1}^2))$. **Left:** B_1, \dots, B_4 are the NBAs of formula $\varphi_1, \dots, \varphi_4$; **Middle:** P_1, \dots, P_4 are the R-posets of B_1, \dots, B_4 ; **Right:** $P_1 \otimes P_2 = \{P_{f1}, P_{f2}\}$, $P_{f3} \in P_{f1} \otimes P_3$ and $P_{f4} \in P_{f3} \otimes P_4$.

A. Task specification and R-poset product

We briefly introduce the syntax of Linear Temporal Logic (LTL) used for task specifications. The basic ingredients of LTL formulas are a set of atomic propositions AP in addition to several Boolean and temporal operators. Atomic propositions are Boolean variables that can be either true or false. The syntax of LTL is defined as: $\varphi \triangleq \top \mid p \mid \varphi_1 \vee \varphi_2 \mid \varphi_1 \wedge \varphi_2 \mid \neg \varphi \mid \bigcirc \varphi \mid \varphi_1 \mathsf{U} \varphi_2 \mid \Box \varphi \mid \Diamond \varphi$ where $\top \triangleq \text{True}$; $p \in AP$ is the alphabet; \vee (*conjunction*), \wedge (*disjunction*), and \neg (*negation*) are the logical operators; \Diamond (*eventually*), \bigcirc (*next*), U (*until*) are the temporal operators; \Box (*always*), \Rightarrow (*implication*) are the derived operators. A special class of LTL formula called *syntactically co-safe* formulas (sc-LTL) [23], [53] only contain the temporal operators \bigcirc , U and \Diamond . A complete description of the semantics and syntax of LTL can be found in [23].

Given a series of sc-LTL formulas that are released online, most existing methods would combine the formulas with \wedge (*conjunction*) and convert them into a Nondeterministic Büchi Automaton (NBA). It results in a graph structure that consists of states, transitions, guards, initial states, and final states. However, since its size is double exponential to the length of formula φ as proven in [42], it quickly becomes intractable with more task formulas. Instead, we compute the product of R-posets associated with these formulas, called the *Poset-prod* (denoted by \otimes). The R-poset $P = (\Omega, \leq, \neq)$ is a high-level abstraction of NBA, proposed in our earlier work [54], which consists of a set of subtasks Ω and their partial relations as less equal \leq and conflict \neq . It has been proven therein that if the subtasks are executed under the partial relations, the resulting traces satisfy the NBA. Once a new task formula is released, it is transformed into a new R-poset P_2 and

its product with the current R-poset P_1 is computed. More specifically, given P_1, P_2 , the Poset-prod returns a new set of R-posets $\mathcal{P} = P_1 \otimes P_2$ that satisfies both P_1 and P_2 , which is computed by iterating the following two procedures:

Task Composition and Relation Update. The first procedure is to create a group of subtasks as a combination between the subtasks in P_2 and the subtasks of P_1 that have not been executed. A depth-first-search algorithm is proposed to gradually add the subtasks along with the corresponding mapping function. The second procedure is to calculate the partial relations between the subtasks such that the ordering constraints among the subtasks in the composed product are consistent without conflicts. Consequently, the overall poset is given by $P_{final} = (\Omega_f, \leq_f, \neq_f)$, which is iteratively computed each time a new poset is added.

The proposed *Poset-prod* method outperforms the tradition method both in computational efficiency and performance. This improvement becomes even more pronounced when the number and length of sub-formulas increase. This is because the time of generating NBAs of $\varphi_1, \varphi_2, \dots$ grows linearly, while the time of converting $\varphi_1 \wedge \varphi_2 \wedge \dots$ into NBA grows exponentially. Moreover, for a new added formula, the algorithm updates the final R-poset based on the previous result, which ensures the performance for online cases. Finally, it is an anytime algorithm that the algorithm can calculate an R-poset within linear complexity for multiple sub-formulas at the expense of optimality. The concrete complexity analysis of *Poset-prod* is shown in Sec. III, and the definition of R-poset and label is shown in Sec. IV.

To give an example, consider four sub-formulas $\varphi_1, \varphi_2, \varphi_3, \varphi_4$ as shown in Fig. 1. Their NBAs $\mathcal{B}_1, \dots, \mathcal{B}_4$ can be transformed into four R-posets P_1, \dots, P_4 . The first round of *Poset-prod* is between P_1 and P_2 as $P_1 \otimes P_2 = \{P_{f1}, P_{f2}\}$. Then, the following rounds of *Poset-prod* are performed between the results of the previous round and the next R-poset as $P_{f1} \otimes P_3$, of which the first solution is denoted by P_{f3} . At the expense of some optimality, the algorithm can go to next round before all results of $P_{f2} \otimes P_3$ are generated, as it is an anytime-algorithm. Finally, we can derive P_{f4} by computing $P_{f3} \otimes P_4$ as the final R-poset which satisfies P_1, \dots, P_4 . Note that the time to generate the NBA associated with $\varphi_1, \bigwedge_{i=1}^2 \varphi_i, \bigwedge_{i=1}^3 \varphi_i$ and $\bigwedge_{i=1}^4 \varphi_i$ grows significantly with a duration of $0.058s, 0.076s, 1.56s, 25.56s$ via LTL2BA [42]. By contrast, the time to compute these products $P_1 \otimes P_2, P_1 \otimes P_2 \otimes P_3, P_1 \otimes P_2 \otimes P_3 \otimes P_4$ grows slower with a duration of $0.199s, 0.279s, 0.385s$. Thus, our method can deal with a much larger number of tasks online. Detailed comparisons between our method and traditional methods can be found in Sec.II-D.

B. Online Subtask Assignment under Complexity Constraints

Once the set of R-posets that satisfies all sub-formulas is generated, a series of subtasks in the R-poset should be assigned to the agents under several complexity constraints, including temporal constraints from R-poset, objects constraints and cooperative constraints. Similar to the classical Contract Net method [55], we propose an efficient and sub-optimal assignment algorithm called Time Bound Contract Net

(TBCN). The main difference is that all these constraints are represented uniformly by time bounds in our methods, and an example is shown in Fig. 2 . The final assignment is a group of timed sequence of robot actions $\mathcal{J} = [J_1, \dots, J_n]$, where $J_n = [(t_k, \omega_k, a_k), \dots]$ indicates that agent n will execute action a_k at time t_k to satisfy subtask ω_k , such that the newly-released tasks are fulfilled.

TBCN consists of three steps: **Initialization, Computation of Feasible Subtasks** and **Online Bidding**. As the partial constraints of final R-poset P_{final} might be changed after computing the product, the subtasks that are conflicting with the updated partial orders are removed in **Initialization**. Then, the last two steps are iterated: the set of subtasks whose partial orders are satisfied given the current assignment \mathcal{J} in **Computation of Feasible Subtasks**; Consequently, a linear program is formulated and solved in the **Online Bidding**, to choose one subtask from the feasible set. Thus, the resulting execution time and action plans are added to \mathcal{J} .

C. Numerical Simulation

As shown in Fig. 4, the hospital environment consists of the wards, the operating rooms, the hall, the exits and the hallways. The multi-agent system is employed with 3 Junior Doctors, 6 Senior Doctors and 8 Nurse, and 4 types of patients are treated as interactive objects including Family Visitors, Vomiting Patients, Senior Patients and Junior Patients. The detailed mappings between agents, action, objects and their labels are shown in Table I. Furthermore, various types of tasks are considered, such as "Go the rounds of the wards and provide medicine", "Check and record the patient status", and "Prepare and perform an operation on a patient". Some tasks are released online under certain conditions. For instance, when a patient vomits at a region, the task "Take the patient into ward and check his status. Meanwhile, the doctors should not enter this region until it has been cleaned". The sc-LTL formula associated with the complete task is given by $\varphi = \varphi_{b1} \wedge \dots \wedge \varphi_{b6} \wedge \varphi_{VP} \wedge \varphi_{JP} \wedge \varphi_{SP}^1 \wedge \varphi_{SP}^2 \wedge \varphi_{FV}$, which has a total length of 62. Detailed description of formulas are shown in Table II.

As shown in Fig. 3, each subtask ω_i consists of the constraints before execution (in blue) and during execution (in green). The directed black arrows denote the ordering constraints, while the bidirectional red arrows for the conflicting constraints. The mapping from the subtasks within the input R-posets to the subtasks within the final R-poset is shown in brackets as $\omega'_1(\omega'_1) : \omega'_1 \rightarrow \omega_1$. Note that most of R-posets on the right are directly incorporated into the final R-posets on the left, such as $P_{b1}, \dots, P_{b6}, P_{u1}, \dots, P_{u5}$. This is due to the fact that their subtasks are independent without ordering constraints, which allows for parallel execution. Additionally, some subtasks on the left represent the same subtasks on the right. For example, ω'_1 of P_{b2} and ω'_1 of P_{b3} representing both ω_5 , since their ordering constraints (in green) are identical. The same action can be performed to satisfy multiple subtasks on the left, which improves the overall efficiency. Furthermore, all subtasks on the right satisfy the partial relations between the corresponding subtasks on the left, while additional constraints

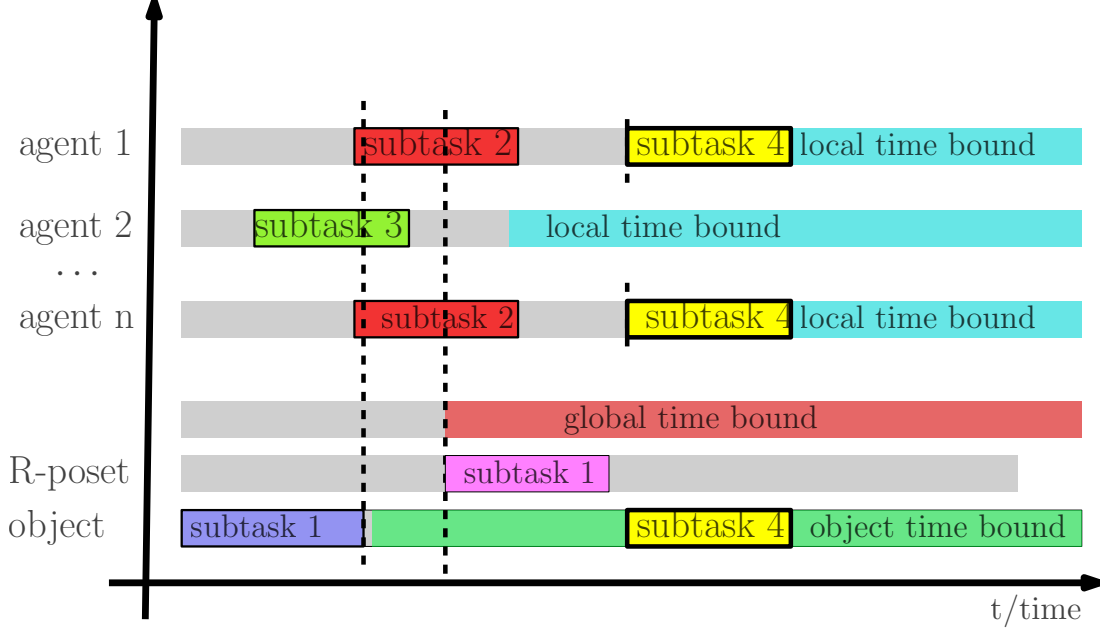


Fig. 2. The bidding process of assigning subtask 4 under the global time bound (when the partial relations in R-poset are satisfied), the time bound for object (when the object is reachable) and local time bounds (when the agents get ready).

are added if there are conflicts among the ordering constraints. For instance, action D_{w_7, w_7}^\emptyset of ω_{15} should not be executed before the subtask ω_{14} . Thus, an additional ordering constraint is added such that subtask ω_{15} should be executed after ω_{14} . These properties guarantee that each subtask within the R-posets on the left can be executed, as their partial relations are satisfied. Consequently, the final R-poset satisfies all R-posets on the left. Note that the complete formula has a total length of 62, of which the NBA takes more than 1h to compute. On the contrary, the first final R-poset is computed within 10.96s.

The results of task assignment are shown in the Fig. 4, which include the updates at 40, 180, 215, 400s with 5 additional objects added. Then, after modifying the current R-posets to accommodate these formulas, the method TBCN is executed to assign the new subtasks within the final R-poset. The trajectories of agents and objects are shown, with certain regions that are not allowed to enter. For instance, when a patient vomits at region $h13$ in Fig. 4 (c), the nurses cannot enter until other agents have cleaned this region. These constraints ensure that both their actions and their trajectories satisfy the R-poset. In addition, once a new object is added, a new formula is released and then the R-poset is updated. All subtasks satisfy the ordering constraints in the R-posets. For instances, as shown in Fig. 4(d), although agents 6, 14 have arrived in region $w7$ before 100s to collaborate on the subtask $\sigma_{16} = \{M_{w7, w7}^\emptyset\}$ (in blue), they have to wait until that agent 10 has fulfilled the subtask $\sigma_{14} = \{C_{w7, w7}^\emptyset\}$, due to the ordering constraints that $(\omega_{14}, \omega_{16}) \in \leq, \{\omega_{14}, \omega_{16}\} \in \neq$. The constraints introduced by objects are also satisfied, e.g., task ω_7 (in green) cannot be executed at 380s before subtask ω_6 (in purple) has been finished, since the required object 3 has not been transferred to region o_4 . Last but not least, most tasks are executed in parallel mostly with a total completion time of 815ss, which is much shorter than 2013.5s if the subtasks

are executed sequentially.

D. Scalability Analysis and Comparisons

First, we show how the computation time of the proposed task assignment method TBCN varies under different numbers of agents and subtasks. Since the number of subtasks cannot be directly determined, we run the TBCN with a large number of formulas, of which the length ranges from 20 to 80. The number of subtasks and the associated computation time are recorded. As shown in Fig. 5, the average computation time only increases slightly as the number of agents is increased from 12 to 400, while the computation time increases considerably if the number of subtasks is increased from 22 to 34. This is due to the fact that new subtasks would introduce additional temporal constraints in the assignment procedure. The execution efficiency η from (6) decreases as the number of agent increases, while η increases slightly as the number of subtasks grows. The highest η is about 39% where most subtasks are executed in parallel with only minimum waiting time for task synchronization.

Secondly, to further validate the scalability of the proposed method against existing methods, we evaluate the time and memory cost to compute both the first R-poset and the complete R-posets by the proposed *Poset-Prod*, given the task formulas of different lengths. The conversion from a LTL formula to NBA is via LTL2BA. The following three baselines are considered: (i) the direct translation from the complete formula to NBA [42], in which the complete formula is the conjunction of all subformulas; (ii) the decomposition-set-based algorithm [56], which decomposes the NBA into independent subtasks; (iii) the sampling-based method [33], [47], which generates a product automaton much smaller than the complete one by sampling the product states of NBA and WTSs via RRT. Each method is tested three times with five

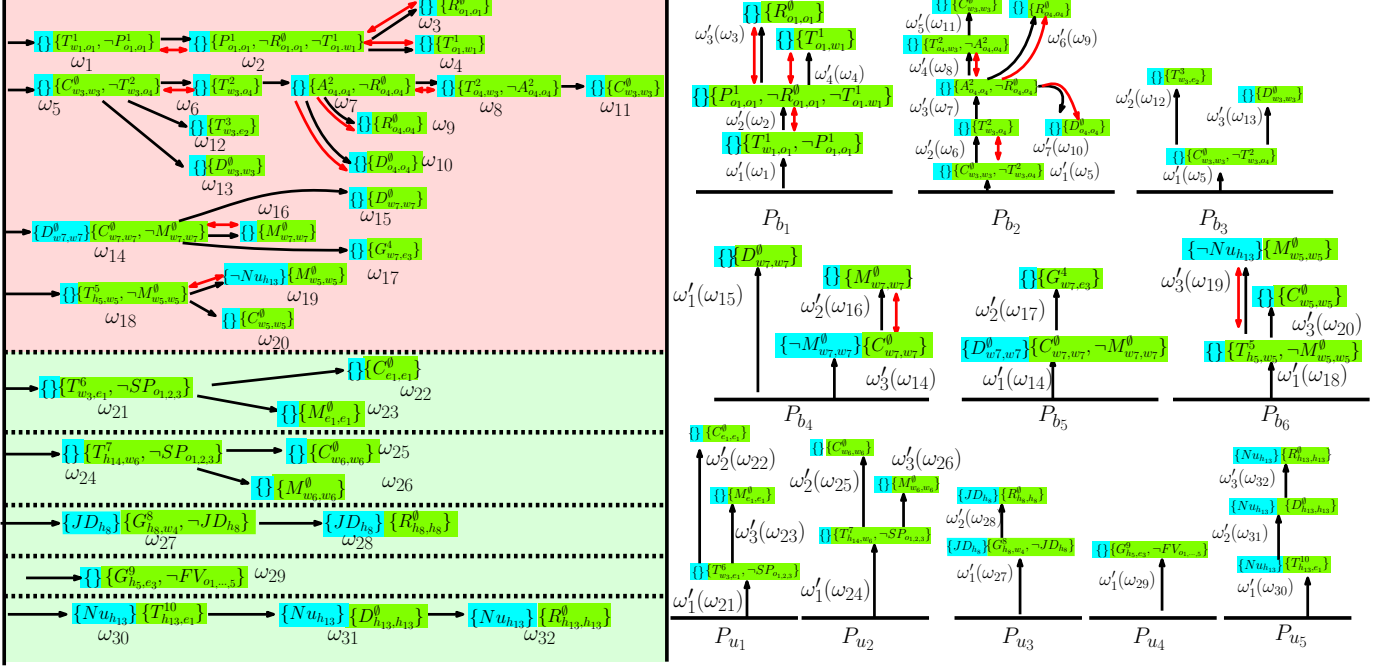


Fig. 3. Illustration of computing the product posets. **Left:** The final R-poset computed from the initial sub-formulas and online sub-formulas (dashed lines); **Right:** P_{b_1}, \dots, P_{b_6} are the R-posets associated with the initial sub-formulas and P_{u_1}, \dots, P_{u_5} are associated with the online sub-formulas.

formulas of the same length ranging from 5 to 400. As shown in Fig. 6, both the time and memory cost increase drastically with the formula length for all methods except the proposed *Poset-prod* to compute the first R-poset. In particular, when the formula length exceeds 15, the decomposition algorithm runs out of memory or time. The sampling-based method can not generate a solution when the formula length exceeds 20. Since all the baseline methods require the translation to NBA first, it becomes intractable as the formula length exceeds 25. In contrast, the proposed method of *Poset-prod* can generate all R-posets with a formula length of 70 and the first R-poset even when the length reaches 400, which is consistent with our analyses in Sec. III.

E. Hardware Experiment

We further tested the proposed method on hardware within a simplified hospital environment. The multi-agent system consists of 10 differential-driven mobile robots, with 3 *JD* in green, 3 *SD* in yellow and 4 *Nu* in blue. The required tasks include "prepare and execute an advanced operation for patient 1 at operating room *o4*". Similar to Sec. II-C, there are event-triggered tasks released online such as "when a patient vomits, take him to the ward, do not enter this region until it is cleaned." The exact task description and formulas are shown in Table. III.

In summary, the system is required with 6 sub-formulas, and the final formula is $\varphi = \varphi_{b1} \wedge \dots \wedge \varphi_{b4} \wedge \varphi_{FV} \wedge \varphi_{JP}$, with the total length 27, thus can not be translated into a NBA directly. The agent trajectories within 185s are shown in Fig. 7. As shown in the right of Fig. 7, the final R-poset consists of 14 subtasks, where the part in red is calculated offline and the part in yellow is generated online. Most subtasks are executed

in parallel, meaning that the R-posets can be satisfied with a high efficiency. The complete R-poset is derived in 3.1s and the task assignment method TBCN is activated three times, of which the average planing time is 2.7s. As shown in the left of Fig. 8, the Gantt graph is updated twice at 5s and 100s during execution, and subtasks that are released online are marked by green boxes. It is worth noting that the agent movement during real execution requires more time due to motion uncertainty, communication delay, drifting and collision avoidance. Nonetheless, the proposed method can adapt to these fluctuations and still satisfy the specified tasks, as shown in the Gantt graph of the overall execution in Fig. 8. Experiment videos are provided in the supplementary files.

III. DISCUSSION

In this work, we propose *Poset-prod*, an efficient online task planning algorithm for multi-agent systems where tasks are released dynamically and constantly online. It consists of a systematic method to convert the temporal tasks into their equivalent R-posets, of which their products are computed online. Given these R-posets, an anytime task assignment algorithm is proposed to adapt the local plans of robots online, such that the overall safety and correctness is ensured. The overall framework is shown to be fast and efficient, thus particularly suitable for large-scale multi-agent systems collaborating in dynamic environments.

The most significant advantage of *Poset-prod* is that the complexity of obtaining the first solution only grows linearly with the length of formulas. Given a set of formulas $\{\varphi_i, i \leq m\}$ and $\max_i |\varphi_i| = n$, deriving the first solution has a polynomial complexity of $O(m^2n^3)$. Despite that the overall complexity to compute the complete R-posets of $\{\varphi_i\}$ is $O(n^{5m})$, it is still much smaller than the complexity of

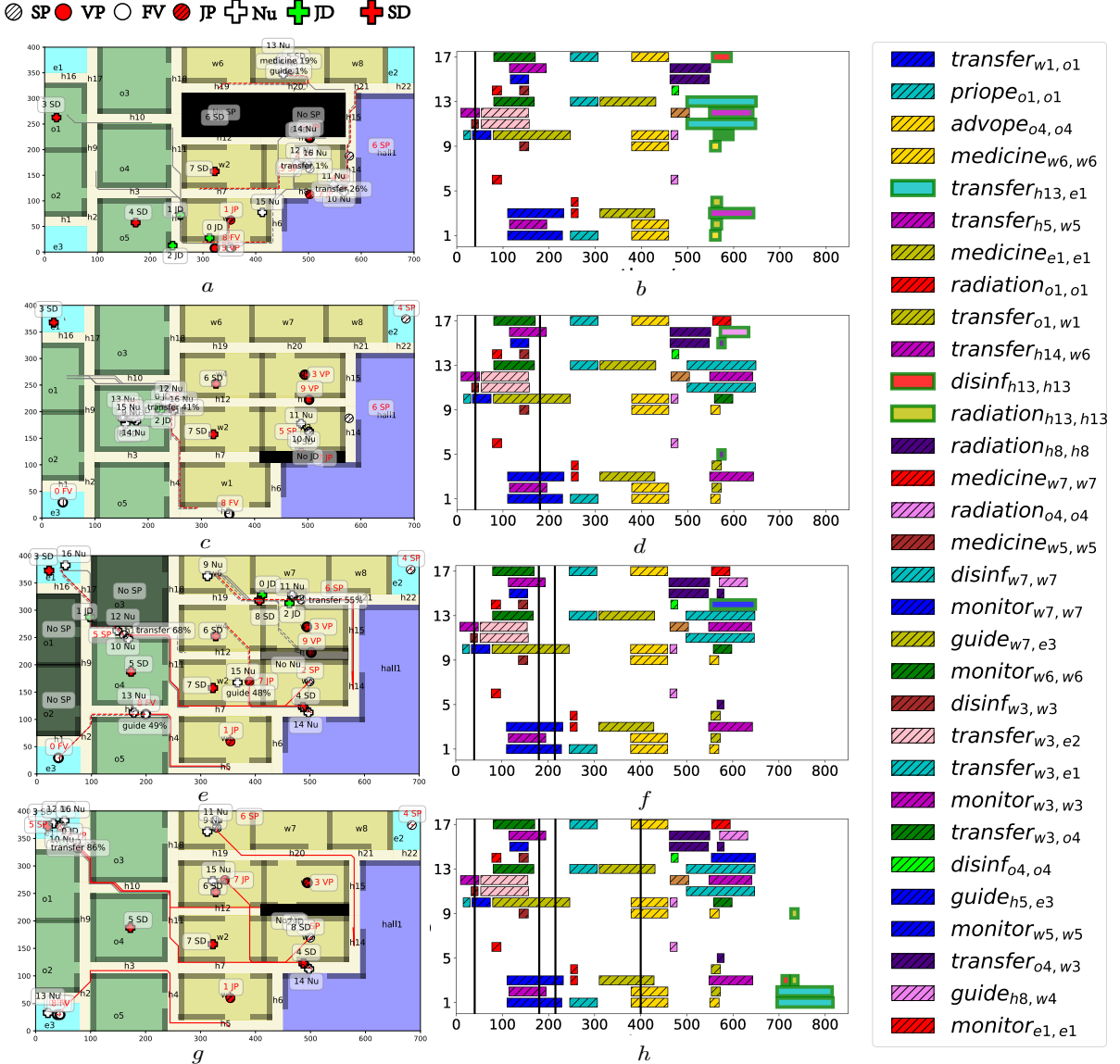


Fig. 4. **Left:** Snapshot of agent trajectories at 40, 180, 215, 400s when new tasks are added online. **Right:** The Gantt graph of task assignment at these time instants, as highlighted in green boxes.

calculating the NBA of the conjunction φ via LTL2BA [42], which is $O(mn \cdot 2^{mn})$. Thus, our method can plan for task formulas with a length of about 400 within about 50s, while most existing methods fail at the formula length of 25.

Future work involves two directions: (i) extending the sc-LTL task formulas to general LTL and other languages such as CTL [24] and STL [25]. It remains unclear how general LTL formulas with *always* operators can be incorporated in the R-poset, especially with the prefix-suffix structure; (ii) considering unknown and uncertain environments that are modeled as Markov Decision Processes (MDP). In this case, a reactive high-level plan is essential to take into account all possible environment behaviors.

IV. MATERIALS AND METHODS

In this section, we provide the knowledge of LTL in Preliminaries, the definition of alphabets and objective function

in problem formulation, and algorithm details in Approach.

A. Preliminaries

As mentioned in Sec.II-A of Result, the basic ingredients of Linear Temporal Logic (LTL) formulas are a set of atomic propositions AP in addition to several Boolean and temporal operators. For a given LTL formula φ , there exists a Non-deterministic Büchi Automaton (NBA) as follows:

Definition 1. A NBA $\mathcal{A} \triangleq (S, \Sigma, \delta, (S_0, S_F))$ is a 4-tuple, where S are the states; $\Sigma = AP$; $\delta : S \times \Sigma \rightarrow 2^S$ are transition relations; $S_0, S_F \subseteq S$ are initial and accepting states.

An infinite word w over the alphabet 2^{AP} is defined as an infinite sequence $W = \sigma_1\sigma_2 \cdots, \sigma_i \in 2^{AP}$. The language of φ is defined as the set of words that satisfy φ , namely, $\mathcal{L}(\varphi) = Words(\varphi) = \{W \mid W \models \varphi\}$ and \models is the satisfaction relation. Additionally, the resulting *run* of w within \mathcal{A} is an infinite

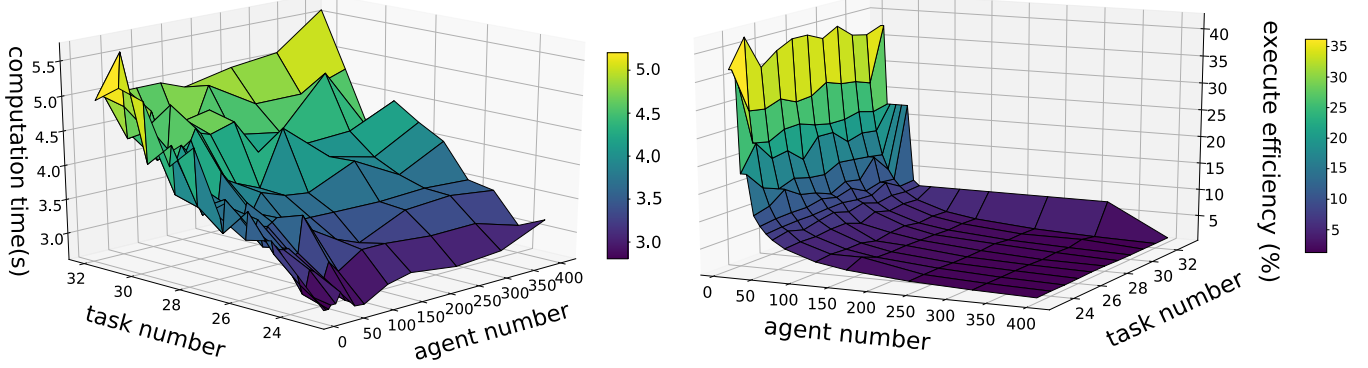


Fig. 5. The computation time (Left) and the execution efficiency η (Right) with respect to different number of agents and subtasks.

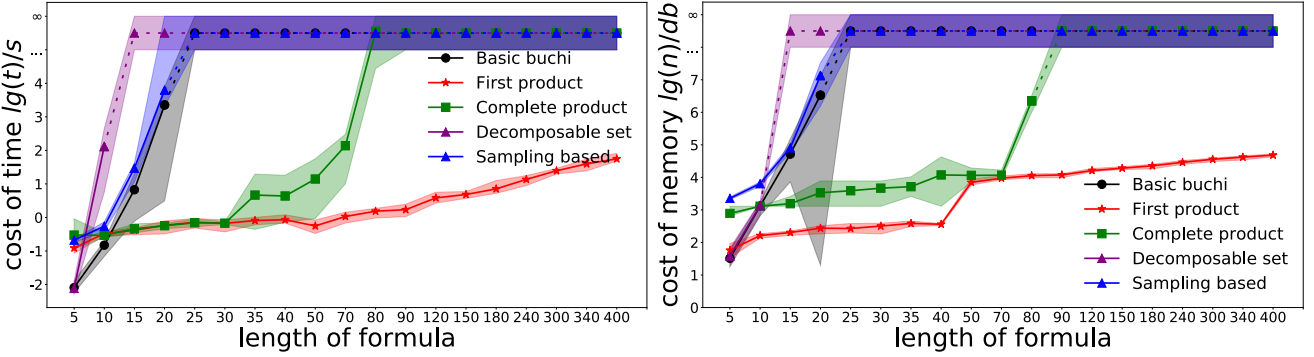


Fig. 6. The comparison of the computation time (Left) and memory (Right) by different methods.

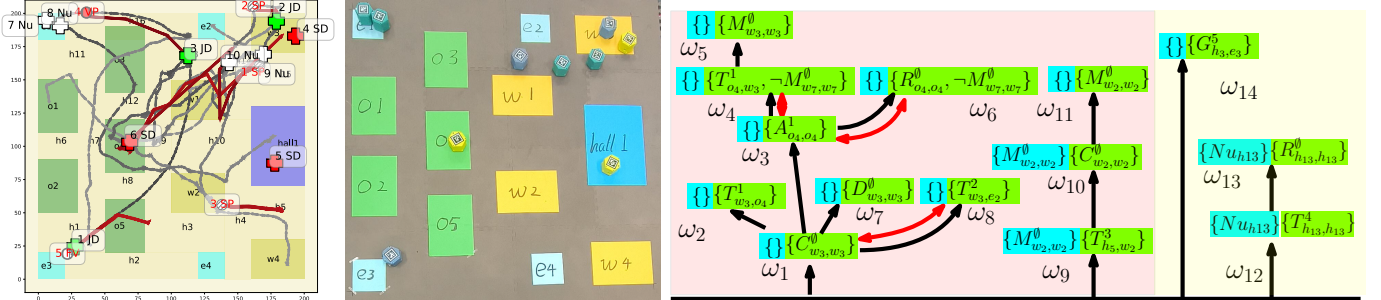


Fig. 7. The trajectories of agents in experiment (Left), experimental snapshot (Middle) and the final R-poset (Right).

sequence $\rho = s_0 s_1 s_2 \dots$ such that $s_0 \in S_0$, and $s_i \in S$, $s_{i+1} \in \delta(s_i, \sigma_i)$ hold for all index $i \geq 0$. A run is called *accepting* if it holds that $\inf(\rho) \cap S_F \neq \emptyset$, where $\inf(\rho)$ is the set of states that appear in ρ infinitely often. A special class of LTL formula called *syntactically co-safe* formulas (sc-LTL) [23], [53], which can be satisfied by a set of finite sequence of words. They only contain the temporal operators \bigcirc , \bigcup and \Diamond and are written in positive normal form where the negation operator \neg is not allowed before the temporal operators. A relaxed partially ordered set (R-poset) over an NBA \mathcal{B}_φ is defined as follows:

Definition 2 (R-poset). [54] R-poset is a 3-tuple: $P_\varphi = (\Omega_\varphi, \leq_\varphi, \neq_\varphi)$: $\Omega_\varphi = \{(\ell, \sigma_\ell, \sigma_\ell^s), \forall \ell = 0, \dots, L\}$ is the set of subtasks, where ℓ is the index of subtask ω_ℓ ; $\sigma_\ell \subseteq \Sigma$

are the transition labels; $\sigma_\ell^s \subseteq \Sigma$ are the self-loop labels from Def. 1 . $\leq_\varphi \subseteq \Omega_\varphi \times \Omega_\varphi$ is the "less equal" relation: If $(\omega_h, \omega_\ell) \in \leq_\varphi$ or equivalently $\omega_h \leq_\varphi \omega_\ell$, then ω_ℓ can only be *started* after ω_h is started. $\neq_\varphi \subseteq 2^{\Omega_\varphi}$ is the "opposed" relation: If $\{\omega_h, \dots, \omega_\ell\} \in \neq_\varphi$ or equivalently $\omega_h \neq_\varphi \dots \neq_\varphi \omega_\ell$, subtasks in $\omega_h, \dots, \omega_\ell$ cannot all be executed simultaneously.

A word is *accepting* if it satisfies all the constraints imposed by P_φ . Additionally, the word of R-poset will satisfy the NBA as $Words(P_\varphi) \subset Words(\varphi)$.

Definition 3 (Language of R-poset). [54] Given a word $w = \sigma'_1 \sigma'_2 \dots$ satisfying R-poset $P_\varphi = (\Omega_\varphi, \leq_\varphi, \neq_\varphi)$, denoted as $w \models P_\varphi$, it holds that: i) given $\omega_{i_1} = (i_1, \sigma_{i_1}, \sigma_{i_1}^s) \in \Omega_\varphi$, there exist j_1 with $\sigma_{i_1} \subseteq \sigma'_{j_1}$ and $\sigma_{j_1}^s \cap \sigma'_{m_1} = \emptyset, \forall m_1 < j_1$; ii) $\forall (\omega_{i_1}, \omega_{i_2}) \in \leq_\varphi, \exists j_1 \leq j_2, \sigma_{i_2} \subseteq \sigma'_{j_2}, \forall m_2 < j_2, \sigma_{j_2}^s \subseteq \sigma'_{m_2}$;

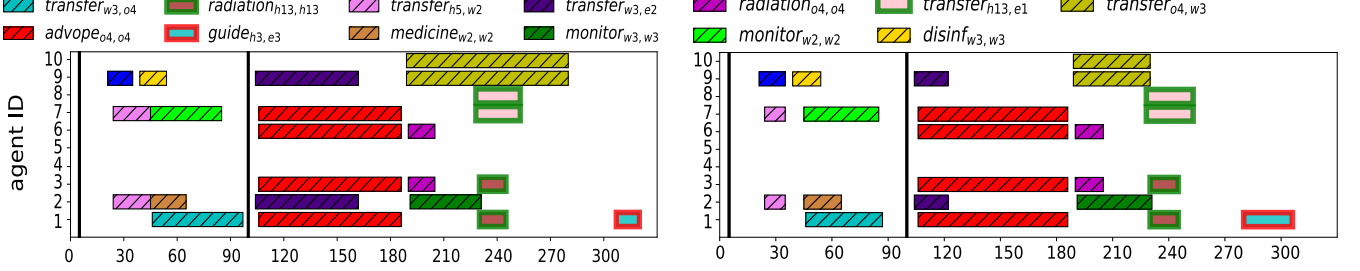


Fig. 8. The Gantt graph of the planned execution (Left) and the Gantt graph of the actual execution (Right).

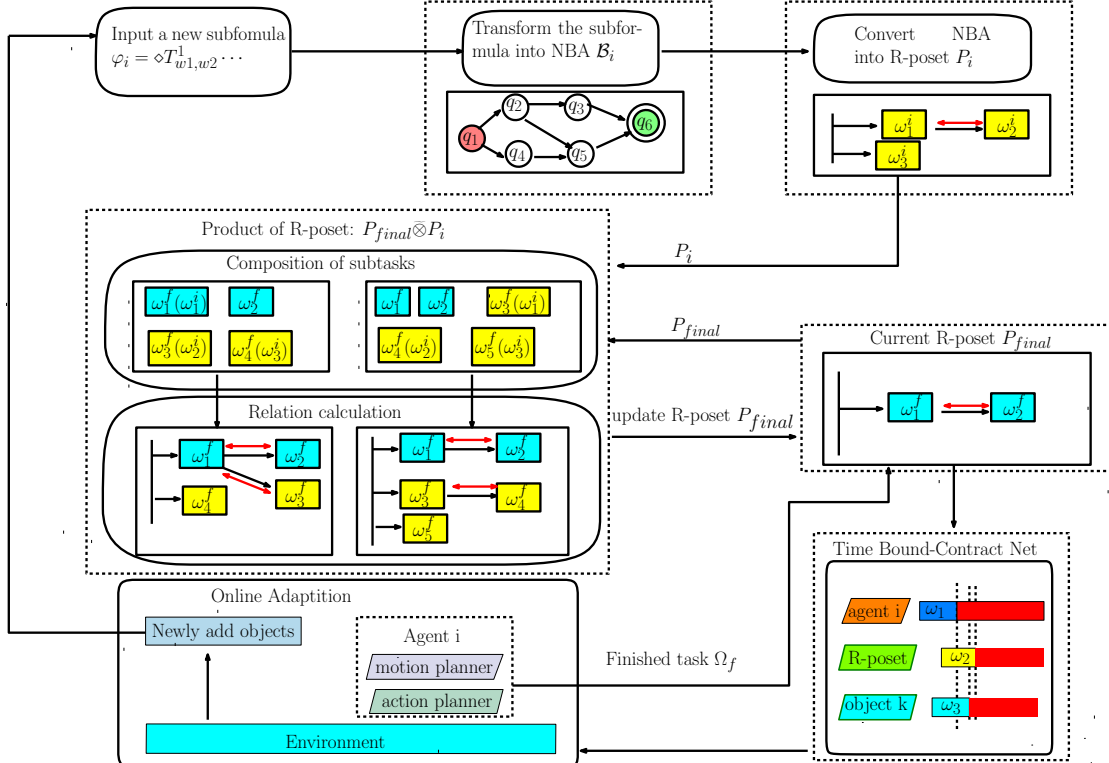


Fig. 9. Framework of the proposed method. For a new input formula φ_i , we firstly change it into an R-poset P_i with the method in Sec. IV-A. Then, Poset-prod between P_i and P_{final} is calculated as in Sec. IV-C1. Thirdly, after the R-poset P_{final} is updated, the TBCN method in Sec. IV-C2 determines and adjusts the task sequence of each agent and object. New tasks are released when the agents execute their local plans and detect new objects online.

iii) $\forall (\omega_{i_1}, \dots, \omega_{i_n}) \in \neq_\varphi, \exists \ell \leq n, \sigma_{i_\ell} \not\subseteq \sigma'_{j_1}$. Language of R-poset P_φ is the set of all word w that satisfies P_φ , denoted by $\mathcal{L}(P_\varphi) \triangleq \{w | w \models P_\varphi\}$.

Assuming that $\mathcal{P}_{b_i} = \{P_1^{b_i}, P_2^{b_i}, \dots\}$ is the set of all possible R-posets of NBA B_{b_i} , it is shown in Lemma 3 of our previous work [54] that: (i) $\mathcal{L}(P_j^{b_i}) \subseteq \mathcal{L}(B_{b_i})$, $P_j^{b_i} \in \mathcal{P}_{\varphi}^{b_i}$; (ii) $\bigcup_{j \in \mathcal{P}_{b_i}} \mathcal{L}(P_j) = \mathcal{L}(B_{b_i})$. In other words, the R-posets contain the necessary information for subsequent steps.

B. Problem Formulation

1) *Collaborative Multi-agent Systems*: Consider a workspace $W \subset \mathbb{R}^2$ with M regions of interest denoted as $\mathcal{W} \triangleq \{W_1, \dots, W_M\}$, where $W_m \in W$. Furthermore, there is a group of agents denoted by $\mathcal{N} \triangleq \{1, \dots, N\}$ with different types $\mathbf{L} \triangleq \{1, \dots, L\}$. More specifically, each agent $n \in \mathcal{N}$ belongs to only one type $l = M_{type}(n)$, where $M_{type} : \mathcal{N} \rightarrow \mathbf{L}$. Each type of agents $l \in \mathbf{L}$ is capable of

providing a set of different actions denoted by \mathcal{A}_l . The set of all actions is denoted as $\mathcal{A}_a = \bigcup_{l \in \mathbf{L}} \mathcal{A}_l = \{a_1, \dots, a_{n_c}\}$. Without loss of generality, the agents can navigate between each region via the same transition graph, i.e., $\mathcal{G} = (\mathcal{W}, \rightarrow_{\mathcal{G}}, d_{\mathcal{G}})$, where $\rightarrow \subseteq \mathcal{W} \times \mathcal{W}$ represents the allowed transitions; and $d_{\mathcal{G}} : \rightarrow_{\mathcal{G}} \rightarrow \mathbb{R}_+$ maps each transition to its duration.

Moreover, there is a set of interactive objects $\mathcal{O} \triangleq \{o_1, \dots, o_U\}$ with several types $\mathcal{T} \triangleq \{T_1, \dots, T_H\}$ scattered across the workspace W . These objects are *interactive* and can be transported by the agents from one region to another. An interactive object $o_u \in \mathcal{O}$ is described by a three-tuple:

$$o_u \triangleq (T_{h_u}, t_u, W_u^p), \quad (1)$$

where $T_{h_u} \in \mathcal{T}$ is the type of object; $t_u \in \mathbb{R}^+$ is the time when o_u appears in workspace W ; $W_u^p : \mathbb{R}^+ \rightarrow \mathcal{W}$ is a function that $W_u^p(t)$ returns the region of o_u at time $t \geq t_u$; and $W_u^p(t_u) \subseteq W$ is the initial region. Additionally, new objects appear in

W over time and are then added to the set \mathcal{O} . With a slightly abusive of notation, we denote the set of initial objects \mathcal{O}_{in} that already exist in W and the set of online objects \mathcal{O}_{on} that are added during execution, i.e., $\mathcal{O} = \mathcal{O}_{in} \cup \mathcal{O}_{on}$.

To interact with the objects, the agents can provide a series of collaborative behaviors $\mathcal{C} \triangleq \{C_1, \dots, C_K\}$. A *collaborative behavior* $C_k \in \mathcal{C}$ is a tuple defined as follows:

$$C_k \triangleq (o_{u_k}, \{(a_i, n_i), i \in \mathbf{L}_k\}) \quad (2)$$

where $o_{u_k} \in \mathcal{O} \cup \{\emptyset\}$ is the interactive object if any; $a_i \in \mathcal{A}_a$ is the set of cooperative actions required; $0 < n_i \leq N$ is the number of agents to provide the action a_i ; and \mathbf{L}_k is the set of action indices associated with the behavior C_k . Also, d_k denotes the execution time of C_k .

A behavior can only be executed if the required object is at the desired region. Since objects can only be transported by the agents, it is essential for the planning process to find the correct order of these transportation behaviors. Related works [57], [50] build a transition system to model the interaction between objects and agents, the size of which grows exponentially with the number of agents and objects.

2) *Task Specifications*: Consider the following two types of atomic propositions: (i) p_m^l is *true* when any agent of type $l \in \mathbf{L}$ is in region $W_m \in \mathcal{W}$; p_m^r is *true* when any object of type $r \in \mathcal{T}$ is in region $W_m \in \mathcal{W}$; Let $\mathbf{p} \triangleq \{p_m^l, \forall W_m \in \mathcal{W}, l \in \mathbf{L}\} \cup \{p_m^r, \forall W_m \in \mathcal{W}, r \in \mathcal{R}\}$. (ii) $(C_k)_{k_1, k_2}^{u_k}$ is *true* when the collaborative behavior C_k in (2) is executed with object o_{u_k} , starting from region W_{k_1} and ending in region W_{k_2} . Let $\mathbf{c} \triangleq \{(C_k)_{k_1, k_2}^{u_k}, \forall C_k \in \mathcal{C}, o_{u_k} \in \mathcal{O}, \forall W_{k_1}, W_{k_2} \in \mathcal{W}\}$. Given these propositions, the team-wise task specification is specified as a sc-LTL formula over $\{\mathbf{p}, \mathbf{c}\}$:

$$\varphi = (\bigwedge_{i \in \mathcal{I}} \varphi_{b_i}) \wedge (\bigwedge_{o_u \in \mathcal{O}_{on}} \varphi_{e_u}), \quad (3)$$

where $\{\varphi_{b_i}, i = 1, \dots, I\}, \{\varphi_{e_u}, o_u \in \mathcal{O}_{on}\}$ are two sets of sc-LTL formulas over $\{\mathbf{p}, \mathbf{c}\}$. The φ_{b_i} is specified in advance while φ_{e_u} is generated online when a new object o_u is added to \mathcal{O}_{on} .

To satisfy the LTL formula φ , the complete action sequence of all agents is defined as

$$\mathcal{J} = (J_1, J_2, \dots, J_N), \quad (4)$$

where $J_n \in \mathcal{J}$ is the sequence of (t_k, C_k, a_k) , which means that agent n executes behavior C_k by providing the collaborative service $a_k \in \mathcal{A}_a$ at time t_k . In turn, the sequences of actions for an interactive object is defined as:

$$\mathcal{J}^o = (J_1^o, J_2^o, \dots, J_U^o), \quad (5)$$

where $J_u^o = (t_k, C_k) \dots$ is the sequence of tasks associated with object $o_u \in \mathcal{O}$. The task pair (t_k, C_k) is added to J_u^o if object o_u joins behavior C_k at time t_k . Assume that the duration of formula $\varphi_{b_i}, \varphi_{e_i}$ from being published to being satisfied is given by D_i , the average efficiency is defined as

$$\eta \triangleq \frac{\sum_{C_k \in J} |\mathbf{L}_k| d_k}{D_i}, \quad (6)$$

which is the percentage of time when actions are performed.

Problem 1. Given the sc-LTL formula φ defined in (3), synthesize and update the motion and action sequence of agents \mathcal{J} and objects \mathcal{J}_o for each agent $n \in \mathcal{N}$ to satisfy φ and maximize execution efficient η .

Although maximizing the task efficiency of a multi-agent system is a classical problem, the combination of interactive objects, long formulas and contingent tasks imposes new challenges in terms of exponential complexity [42], [50] and online adaptation [51].

C. Approach

As shown in Fig. 9, when a new R-poset is generated, the proposed solution realizes the requirement through two main components: i) Product of R-posets, where the product of existing R-posets is computed incrementally; ii) Task assignment, where subtasks are assigned to the agents given the temporal and spatial constraints specified in the R-poset.

1) *Product of R-posets*: As the first two steps showed in Fig. 9, when a new formula $\varphi_i \in \Phi_b, \Phi_u$ is added, it will be transform into NBA first. Then, an R-poset P_i is generated by the method proposed in our previous work [54]. The other R-poset P_{final} involved in calculation is the previous result of *Poset-prod*, which will be updated after this round calculation. With P_{final} as $P_1 = (\Omega_1, \leq_1, \neq_1)$, P_i as $P_2 = (\Omega_2, \leq_2, \neq_2)$, we define product of R-posets as follows:

Definition 4 (Product of R-posets). Given a finite word w_0 , the product of two R-posets P_1, P_2 is defined as a set of R-posets $\mathcal{P}^r = \{P'_1, P'_2, \dots\}$, denoted as $\mathcal{P}^r = P_1 \otimes P_2$ where P'_i satisfies two conditions: (i) if $w_0 w \in \mathcal{L}(P_1), w \in \mathcal{L}(P_2)$, then $w_0 w \in \bigcup_{P'_i \in \mathcal{P}^r} \mathcal{L}(P'_i)$; (ii) if $w_0 w \in \mathcal{L}(P'_i)$, $P'_i \in \mathcal{P}^r$, then $w_0 w \in \mathcal{L}(P'_i), w \in \mathcal{L}(P_2)$.

The word w_0 is already executed, containing the finished subtasks Ω_{finish}^1 of P_1 . Thus, w_0 can not influence P_2 whose subtasks will be executed in the future. Specially, if the new formula is offline as $\varphi_i \in \Phi_b$ and the agents have not started to execute subtasks, w_0 will be set as empty. As showed in Fig. 9, *Poset-prod* consists of following two steps.

(i) **Task Composition**. In this step, we generate all possible combinations of subtasks which can satisfy both Ω_1 and Ω_2 . Namely, a set of subtasks $\Omega' = \{\omega'_1, \dots, \omega'_{n'}\}$ satisfies Ω_1 if for each $\omega_i^1 = (i, \sigma_i^1, \sigma_i^{s1}) \in \Omega_1$, there is a subtask $\omega_j' = (j, \sigma_j', \sigma_j^{s'}) \in \Omega'$ satisfying $\sigma_i^1 \subseteq \sigma_j'$ and $\sigma_i^{s1} \subseteq \sigma_j^{s'}$, or $\omega_j' \models \omega_i^1$ for brevity. Thus, we set $\Omega' = \Omega_1$ firstly and Ω' clearly satisfies Ω_1 with $\forall \omega_i^1 \in \Omega_1, \omega_i' \models \omega_i^1$. Then, a mapping function $M_\Omega : \Omega_2 \rightarrow \Omega'$ is defined to store the satisfying relationship from Ω_2 to Ω' , and $\mathcal{D}(M_\Omega) \in \Omega_2$ is the domain of M_Ω , $\mathcal{R}(M_\Omega)$ is the range of M_Ω . As all relations are unknown, M_Ω , $\mathcal{D}(M_\Omega)$ and $\mathcal{R}(M_\Omega)$ are initially set to empty. Namely, if $\omega_j' \models \omega_i^2$, we will store $M_\Omega(\omega_i^2) = \omega_j'$ and $M_\Omega^{-1}(\omega_j') = \omega_i^2$, and add ω_i^2 into $\mathcal{D}(M_\Omega)$, ω_j' into $\mathcal{R}(M_\Omega)$, where M_Ω^{-1} is the inverse function of M_Ω .

A depth-first-search (DFS) [58] is used to add the subtasks of Ω_2 to Ω' in order and these mapping relations will be recorded in M_Ω . The search sequences of DFS can be initialized as $que = [(\Omega' = \Omega_1, M_\Omega = \emptyset)]$. Then, during the circle, we will fetch the first node of que as (Ω', M_Ω') . The

next unmixed subtasks in Ω_2 is $\omega_i^2, i = |M'_\Omega| + 1$. Any subtask $\omega_j^1 \in \Omega_1/R(M'_\Omega)/\Omega_{finish}^1$ with $\omega_j^1 \models \omega_i^2$ or $\omega_i^2 \models \omega_j^1$ can create a new combination based on (Ω', M'_Ω) :

$$\begin{aligned}\hat{\Omega}' &= \Omega', \hat{\omega}'_j = (j, \sigma_j^1 \cup \sigma_i^2, \sigma_j^{s1} \cup \sigma_i^{s2}), \\ M'_\Omega &= M'_\Omega, \hat{M}'_\Omega(\omega_i^2) = \omega'_j,\end{aligned}\quad (7)$$

which means the subtask ω'_j in Ω' can satisfy both ω_j^1, ω_i^2 . Moreover, for the subtask ω_i^2 , we can always create a set of subtasks $\hat{\Omega}'$ and the corresponding mapping function \hat{M}'_Ω by appending ω_i^2 into Ω' as $\hat{\omega}'_j$ such that $\hat{\omega}'_j \models \omega_i^2$ holds, i.e.,

$$\begin{aligned}\hat{\Omega}' &= \Omega', j = |\Omega'| + 1, \hat{\omega}'_j = \omega_i^2; \\ \hat{M}'_\Omega &= M'_\Omega, \hat{M}'_\Omega(\omega_i^2) = \omega'_j,\end{aligned}\quad (8)$$

which means the subtask ω'_j can be executed to satisfy ω_i^2 . This step ends if the time budget t_b or the search sequence que exhausted. Once $|D(M'_\Omega)| = |\Omega_2|$, a Ω' satisfying Ω_1, Ω_2 is already found. In this case, the next step is triggered. As showed in Fig. 9, one of found combination is $M_\Omega^1(1) = 1, M_\Omega^1(3) = 2, M_\Omega^1(4) = 3$, and ω_1^f is created by (7), and ω_3^f, ω_4^f is created by (8).

(ii) **Relation Update.** Given the set of subtasks Ω' and the mapping function M_Ω , we calculate the partial relations among them and build a product R-poset P . Firstly, we construct the “less-equal” constraint \leq as follows:

$$\leq = \leq_1 \cup \{(M_\Omega(\omega_{\ell_1}^2), M_\Omega(\omega_{\ell_2}^2)) | (\omega_{\ell_1}^2, \omega_{\ell_2}^2) \in \leq_2\}, \quad (9)$$

which inherits both less equal relations \leq_1 in P_1 and \leq_2 in P_2 . Then, we update Ω' to consider the constraints imposed by the self-loop labels in other subtasks. Specifically, if a new relation (ω_i, ω_j) is added to \leq by $(M_\Omega^{-1}(\omega_i^2), M_\Omega^{-1}(\omega_j^2)) \in \leq_2$ while $(\omega_i^1, \omega_j^1) \notin \leq_1$ holds, ω_i is required to be executed before ω_j although (ω_i^1, ω_j^1) does not belong to \leq_1 of P_1 . In this case, σ_i and σ_i^s are updated to guarantee the satisfaction of the self-loop labels σ_j^s before executing σ_j . For each subtask ω_i , the newly-added suf-subtasks from \leq_1, \leq_2 are defined as S_p^1, S_p^2 , i.e.,

$$\begin{aligned}S_p^1 &= \{\omega_j | (\omega_i, \omega_j) \in \leq, (\omega_i^1, \omega_j^1) \notin \leq_1\}, \\ S_p^2 &= \{M_\Omega^{-1}(\omega_j) | (\omega_i, \omega_j) \in \leq, (M_\Omega^{-1}(\omega_i^2), M_\Omega^{-1}(\omega_j^2)) \notin \leq_2\},\end{aligned}\quad (10)$$

where are the subtasks that should be executed after ω_i . Thus, the action labels σ_i and self-loop labels σ_i^s in $\omega_i = (i, \sigma_i, \sigma_i^s)$ are updated accordingly as follows:

$$\hat{\sigma} = \bigcup_{\omega_\ell^1 \in S_p^1} \sigma_\ell^{s1} \cup \bigcup_{\omega_\ell^2 \in S_p^2} \sigma_\ell^{s2}, \sigma_i^s = \hat{\sigma} \cup \sigma_i^s, \sigma_i = \hat{\sigma} \cup \sigma_i, \quad (11)$$

in which σ_i^s and σ_i should be executed under the additional labels $\hat{\sigma}$ thus the self-loop labels of S_p^1, S_p^2 are satisfied.

Finally, we find the potential ordering by checking whether a subtask σ_i^s is in conflicts with another subtask σ_j while $(\omega_i, \omega_j) \notin \leq$. If so, an additional ordering (ω_i, ω_j) will be added to \leq as:

$$\leq = \leq \cup \{(\omega_i, \omega_j) | \sigma_j \models \sigma_i^s\} \quad (12)$$

Then, Ω will be updated following (10) and (11). Regarding the set of subtasks Ω that have no conflicts in \leq , its “not-equal” relations \neq is generated by a simple combination as:

$$\neq = \neq_1 \cup \left\{ \{M_\Omega(\omega_{\ell_i})\} | \{\omega_{\ell_i}\} \in \neq_2 \right\}. \quad (13)$$

The resulting poset $P_i = (\Omega, \leq, \neq)$ is added to \mathcal{P}_{final} .

As shown in Fig. 9, **Relation Update** gets two R-posets and the partial relations of each R-poset are succeeded from P_i, P_{final} . Due to the anytime property, the two steps procedure can be repeated until all possible R-posets are found or just ended when the first R-poset is found.

2) **Task Assignment:** To satisfy the final R-poset $P_{final} = (\Omega_f, \leq_f, \neq_f)$, the subtasks Ω_f should be executed under the partial orders of \leq_f, \neq_f . Each subtask $\omega_i \in \Omega_c$ represents a collaborative behavior C_j . Thus, we can redefine the action sequence of each agent $J_n \in \mathcal{J}$ as $J_n = [(t_k, \omega_k, a_k), \dots]$ and the action sequence of each object $J_u^o \in \mathcal{J}_o$ as $J_u^o = [(t_k, \omega_k, a_k), \dots]$, in which we replace the cooperative behavior C_k with ω_k since $C_k \in \sigma_k$.

We propose a sub-optimal algorithm called Time Bound Contract Net (TBCN) to generate and adapt the action sequence of agents and objects. Compared with the classical Contract Net method [55], the main differences are: (i) the partial order \leq_f, \neq_f of R-poset might be changed when new formula added, (ii) the assigned subtasks should satisfy the partial orders in \leq_f, \neq_f ; (iii) the cooperative task should be fulfilled by multiple agents; and (iv) interactive objects should be considered as an additional constraints. TBCN solves these differences with three steps: Firstly, we design a cancellation mechanism in the initialization to adapt to the changes of R-poset mentioned in (i). Secondly, the partial orders in (ii) are guaranteed by only assigning feasible subtasks but not all unassigned subtasks in each loop. Thirdly, the constraints mentioned in (iii) and (iv) are considered as a time bound $t_1 \in \mathbb{R}^+$ in the bidding process.

(i) **Initialization:** Once the R-poset P_{final} is update by *Poset-prod*, we firstly collect the action sequence $\mathcal{J}, \mathcal{J}_o$ of previous solution and the set of finished subtasks Ω_{finish} from executing word w_0 . Specially, all of them will be empty if it is the first round. Then, a set of essential conflict subtasks Ω_{ec} is defined to collect the subtasks which might conflicts the updated partial orders \leq_f, \neq_f :

$$\begin{aligned}\Omega_{ec} = \{ &\omega_i | \omega_i \leq_f \omega_j, t_i \geq t_j, \forall \omega_i, \omega_j \in \Omega_1/\Omega_{finish} \} \cup \\ &\{ \omega_i | \omega_i \neq_f \omega_j, t_j \leq t_i \leq t_j + d_j, \\ &\forall \omega_i, \omega_j \in \Omega_1/\Omega_{finish} \}.\end{aligned}\quad (14)$$

Then, we compute the set of subtasks Ω_{conf} that should be removed from $\mathcal{J}, \mathcal{J}_o$:

$$\Omega_{conf} = \{ \omega_j | \omega_i \leq_f \omega_j, \forall \omega_i \in \Omega_1/\Omega_{finish}, \\ \forall \omega_j \in \Omega_{ec} \} \cup \Omega_{ec}, \quad (15)$$

in which are the subtasks in Ω_{ec} and the subtasks whose pre-subtasks will be removed. With the action sequences $\mathcal{J}, \mathcal{J}_o$ removed all the subtasks in Ω_{conf} , we can initialize the set of assigned subtasks $\Omega_{as} = \{\omega_i | \forall (t_i, \omega_i, a_i) \in \mathcal{J}\}$ and the set of unassigned subtasks $\Omega_u = \Omega_f/\Omega_{as}$.

(ii) **Computation of Feasible Subtasks:** After initialization, the algorithm starts a loop to assigned the subtasks in Ω_u : getting a set of feasible subtasks Ω_{fe} ; calculating their time bounds; choosing the best subtask. For the ordering constraints \leq_c , if $(\omega_j, \omega_i) \in \leq_c$, assigning $(t_{kj}, \omega_j, a_{kj})$ to a task sequence

$J_i = \dots (t_{k_i}, \omega_i, a_{k_i})$ will violate such constraints. Thus, the Ω_{fe} based on current Ω_{as} is defined as:

$$\Omega_{fe} = \{\omega_i | \omega_i \in \Omega_u, \forall (\omega_j, \omega_i) \in \leq_f, \omega_j \in \Omega_{as}\}, \quad (16)$$

in which the subtasks may lead to unfeasible action sequences being eliminated.

(iii) **Online Bidding**: Then, we will try assigning each subtask in Ω_{fe} and only choose the one with the best result. Without loss of generality, we assume that subtask $\omega_i \in \Omega_{fe}$ requires a label $(C_k)_{k_1, k_2}^{u_k}$, which means the agents need to execute the behavior C_k from region W_{k_1} to region W_{k_2} using object u_k . Any constraint mentioned in (ii), (iii) and (iv) can be considered as a time bound $t_1 \in \mathbb{R}^+$ which means such constraint can be satisfied after t_1 . Here, we use three kinds of time bounds: the global time bound t_i^ω , the object time bound $t_{u_k}^o$ and the set of local time bounds T_s . The global time bound t_i^ω is the time instance that the ordering constraints \leq_f and conflict constraints \neq_f will be satisfied if behavior $(C_k)_{k_1, k_2}^{u_k}$ is executed after t_i^ω :

$$\begin{aligned} t_i^\omega &\geq t_j, \forall (j, i) \in \leq_f, \omega_j \in \Omega_{as}, \\ t_i^\omega &\geq t_\ell + d_\ell, \forall \{\omega_i, \omega_\ell, \dots\} \in \neq_f, \omega_\ell \in \Omega_{as}. \end{aligned} \quad (17)$$

For the required object u_k , assuming its participated last task is $\mathcal{J}_{u_k}^o[-1] = (t_\ell, \omega_\ell)$, the object time bound $t_{u_k}^o$ should satisfy that:

$$W_u^p(t) = W_{k_1}, t \geq t_\ell + d_\ell, \forall t \geq t_{u_k}^o, \quad (18)$$

which means the object u_k will be at the starting region W_{k_1} of the current behavior $(C_k)_{k_1, k_2}^{u_k}$ and ready for it after $t_{u_k}^o$. Additionally, we set $t_{u_k}^o = \infty$ if the object is not at W_{k_1} after the action sequence $\mathcal{J}_{u_k}^o$, and we set $t_{u_k}^o = 0$ if the behavior $(C_k)_{k_1, k_2}^{u_k}$ does not require object as $u_k = \emptyset$. The set of local time bound is defined as

$$\begin{aligned} T_s &= \{(\mathcal{A}_n, t_n^a) | \mathcal{A}_n = \mathcal{A}_{M_{type}(n)} \cap \mathcal{A}_{C_k}, \\ t_n^a &= t_\ell + d_\ell + d_g(k_\ell, k_1), \forall n \in \mathcal{N}\}, \end{aligned} \quad (19)$$

where \mathcal{A}_n is the set of actions that agent n can provide for behavior C_k , t_n^a is the earliest time agent n can arrive region W_{k_1} , $t_\ell + d_\ell$ is the time when the last subtask $\omega_\ell \in J_n[-1]$ has finished, $d_g(k_\ell, k_1)$ is the cost of moving and W_{k_ℓ} is the goal region of ω_ℓ . (\mathcal{A}_n, t_n^a) means agent n can begin behavior $(C_k)_{k_1, k_2}^{u_k}$ after time t_n^a by providing one of action $a_\ell \in \mathcal{A}_n$. Using these time bounds, we can determine the agents and their providing actions and generate a new party assignment $\mathcal{J}^i, \mathcal{J}_o^i$ to minimize the ending time of subtask ω_i . The efficiency η of each assignment $\mathcal{J}^i, \mathcal{J}_o^i, \omega_i \in \Omega_u$ is calculated, and the subtask with max efficiency will be chosen. Afterwards, the chosen subtask is removed from Ω_{un} and added to Ω_{as} . The action sequences $\mathcal{J}, \mathcal{J}_o$ are updated accordingly as $\mathcal{J} = \mathcal{J}^i, \mathcal{J}_o = \mathcal{J}_o^i$ for the next iteration.

D. Correctness and Completeness Analysis

Theorem 1 (Correctness). *Given two R-posets $P_1 = (\Omega_1, \leq_1, \neq_1), P_2 = (\Omega_2, \leq_2, \neq_2)$ generated from $\mathcal{B}_1, \mathcal{B}_2$, we have $\mathcal{L}(P_j) \subseteq \mathcal{L}(P_1) \cap \mathcal{L}(P_2)$, where $P_j \in \mathcal{P}_{final}$, $\mathcal{P}_{final} = P_1 \otimes P_2$.*

Proof. If a word $w = \sigma'_1 \sigma'_2 \dots$ satisfies $P_j = (\Omega_j, \leq_j, \neq_j)$, $P_j \in \mathcal{P}_{final}$, it satisfies the three conditions mentioned in Def. 3. In first condition, due to the step **Task Composition** of **Poset-prod**, we can infer that for any $\omega_n^1 = (n, \sigma_n^1, \sigma_n^{s1}) \in \Omega_1$, there exists $\omega_n = (n, \sigma_n, \sigma_n^s) \in \Omega_j$, with $\sigma_n^1 \subseteq \sigma_n, \sigma_n^{s1} \subseteq \sigma_n^s$. Thus, we have $\sigma_{i_1}^1 \subseteq \sigma_{i_1} \subseteq \sigma'_{\ell_1}$ and $\sigma_{i_1}^{s1} \cap \sigma'_{m_1} = \emptyset, \forall m_1 < \ell_1$, which indicates that w satisfies P_1 for condition 1. For the second condition, due to (9) in step **Relation Update**, we have $\leq_i \subseteq \leq_j$. Thus, we can infer that w satisfies P_1 for the second condition: Any $(\omega_{i_1}^1, \omega_{i_2}^1) \in \leq_1$, we have $(\omega_{i_1}, \omega_{i_2}) \in \leq_j$, thus $\exists \ell_1 \leq \ell_2, \sigma_{i_2}^1 \subseteq \sigma_{i_2} \subseteq \sigma'_{\ell_2}$, and $\forall m_2 < \ell_2, \sigma_{\ell_2}^{s1} \subseteq \sigma_{\ell_2}^s \subseteq \sigma'_{m_2}$. Additionally, for the last condition, as the word w satisfied the \neq_j order of P_j . We have $\neq_1 \subseteq \neq_j$ due to (13). Thus, the word w also satisfied the third condition. In the end, we can conclude that w satisfies P_1 . In the same way, we can proof the w also satisfies P_2 . Thus, $\mathcal{L}(P_j) \subseteq \mathcal{L}(P_1) \cap \mathcal{L}(P_2)$ \square

Theorem 2 (Completeness). *Given two R-posets P_1, P_2 getting from $\mathcal{B}_1, \mathcal{B}_2$, with enough time budget, Poset-prod returns a set \mathcal{P}_{final} consisting of all final product, and its language $\mathcal{L}(\mathcal{P}_{final}) = \bigcup_{P_i \in \mathcal{P}_{final}} \mathcal{L}(P_i)$ is equal to $\mathcal{L}(\mathcal{P}_{final}) = \mathcal{L}(P_1) \cap \mathcal{L}(P_2)$.*

Proof. Due to Theorem 1, it holds that $\mathcal{L}(\mathcal{P}_{final}) \subseteq \mathcal{L}(P_1) \cap \mathcal{L}(P_2)$. Thus, we only need to show that $\mathcal{L}(P_1) \cap \mathcal{L}(P_2) \subseteq \mathcal{L}(\mathcal{P}_{final})$. Given a word $w = \sigma'_1 \sigma'_2 \dots$ and $w \in \mathcal{L}(P_1) \cap \mathcal{L}(P_2)$, w satisfies the first condition in Def. 3 for both P_1 and P_2 that: $\forall \omega_{i_1}^1 = (i_1, \sigma_{i_1}^1, \sigma_{i_1}^{s1}) \in \Omega_1$, there exists σ'_{j_1} with $\sigma_{i_1}^1 \subseteq \sigma'_{j_1}$ and $\sigma_{i_1}^{s1} \subseteq \sigma'_{m_1}, \forall m_1 < j_1$; $\forall \omega_{i_2}^2 = (i_2, \sigma_{i_2}^2, \sigma_{i_2}^{s2}) \in \Omega_2$, there exists σ'_{j_2} with $\sigma_{i_2}^2 \subseteq \sigma'_{j_2}$ and $\sigma_{i_2}^{s2} \subseteq \sigma'_{m_2}, \forall m_2 < j_2$. If $j_1 = j_2$, the step in (8) of **Task Composition** will generate a subtask $\omega_{i_1} \in \Omega_j$ with $\omega_{i_1} \models \omega_{i_1}^1, \omega_{i_2}^2$, and $\sigma_{i_1} \subseteq \sigma'_{j_1}, \forall m_3 < j_1, \sigma_{j_1}^s \subseteq \sigma'_{m_3}$. If $j_1 \neq j_2$, the (7) will generate $\omega_{M_\Omega(i_2)} \models \omega_{i_2}^2$, with $\sigma_{M_\Omega(i_2)} \subseteq \sigma'_{j_2}, \forall m_4 < j_2, \sigma_{M_\Omega(i_2)}^s \subseteq \sigma'_{m_4}$. Thus, there exists $P_j \in \mathcal{P}_{final}$ that satisfies the first condition. For the second condition, \leq_j consisting of two parts generated by (9) and (12) guarantees that $w \in \mathcal{L}(P_1) \cap \mathcal{L}(P_2)$. Moreover, (10) and (11) guarantee that w does not conflict the self-loop constraints of P_1, P_2 . Thus, the second condition is satisfied. Regarding the third condition, since $\neq_j = \neq_1 \cap M_\Omega(\neq_2)$ holds in (13), \neq_j is naturally satisfied by w . In conclusion, for any $w \in \mathcal{L}(P_1) \cap \mathcal{L}(P_2)$, $w \in \mathcal{L}(\mathcal{P}_{final})$ holds and vice versa. Thus, $\mathcal{L}(\mathcal{P}_{final})$ is equal to $\mathcal{L}(P_1) \cap \mathcal{L}(P_2)$. \square

ACKNOWLEDGMENTS

Author Contributions

Z. Li and M. Guo initiated the idea. Z. Liu designed the algorithms and conducted the experiments. Z. Liu and M. Guo wrote the first draft of the manuscript. Z. Liu, M. Guo, W. Bao and Z. Li commented and revised the manuscript. Z. Li and W. Bao supervised the work. All authors have read, commented, and approved the final manuscript.

Funding

This work was supported by the National Key R&D Program of China under grants 2022ZD0116401 and 2022ZD0116400, the National Natural Science Foundation

of China under grants U2241214, 62373008, 62203017, and T2121002.

Conflicts of Interest

The authors declare that there is no conflict of interest regarding the publication of this article.

Data Availability

The authors confirm that the data supporting the findings of this study are available within the article.

REFERENCES

- [1] H. Jemal, Z. Kechaou, M. B. Ayed, and A. M. Alimi, “A multi agent system for hospital organization,” *International Journal of Machine Learning and Computing*, vol. 5, no. 1, pp. 51–56, 2015.
- [2] O. M. Cliff, R. Fitch, S. Sukkarieh, D. L. Saunders, and R. Heinsohn, “Online localization of radio-tagged wildlife with an autonomous aerial robot system,” in *Robotics: Science and Systems*, 2015.
- [3] C. Zhang, A. Hammad, and H. Bahnassi, “Collaborative multi-agent systems for construction equipment based on real-time field data capturing,” *Journal of Information Technology in Construction (ITcon)*, vol. 14, no. 16, pp. 204–228, 2009.
- [4] T. Arai, E. Pagello, L. E. Parker *et al.*, “Advances in multi-robot systems,” *IEEE Transactions on Robotics and Automation*, vol. 18, no. 5, pp. 655–661, 2002.
- [5] P. Toth and D. Vigo, “An overview of vehicle routing problems,” *The Vehicle Routing Problem*, pp. 1–26, 2002.
- [6] J. Fink, M. A. Hsieh, and V. Kumar, “Multi-robot manipulation via caging in environments with obstacles,” in *2008 IEEE International Conference on Robotics and Automation*, 2008, pp. 1471–1476.
- [7] P. Arm, G. Waibel, J. Preisig, T. Tuna, R. Zhou, V. Bickel, G. Ligeza, T. Miki, F. Kehl, H. Kolenbach, and M. Hutter, “Scientific exploration of challenging planetary analog environments with a team of legged robots,” *Science Robotics*, vol. 8, no. 80, p. eade9548, 2023.
- [8] A. Varava, K. Hang, D. Kragic, and F. T. Pokorny, “Herdling by caging: a topological approach towards guiding moving agents via mobile robots,” in *Robotics: Science and Systems*, 2017, pp. 696–700.
- [9] Y. Ozkan-Aydin and D. I. Goldman, “Self-reconfigurable multilegged robot swarms collectively accomplish challenging terrodynamic tasks,” *Science Robotics*, vol. 6, no. 56, p. eabf1628, 2021.
- [10] W. Ruan, H. Duan, Y. Sun, W. Yuan, and J. Xia, “Multiplayer reach-avoid differential games in 3d space inspired by harris’ hawks’ cooperative hunting tactics,” *Research*, vol. 6, p. 0246, 2023.
- [11] S. Kartik and C. Siva, Ram Murthy, “Task allocation algorithms for maximizing reliability of distributed computing systems,” *IEEE Transactions on Computers*, vol. 46, no. 6, pp. P.719–724, 1997.
- [12] P. Agrawal, P. Varakantham, and W. Yeoh, “Scalable greedy algorithms for task/resource constrained multi-agent stochastic planning,” in *Proceedings of the 25th International Joint Conference on Artificial Intelligence IJCAI 2016: New York, July 9*, vol. 15, 2016, pp. 10–16.
- [13] B. Keshanchi, A. Souri, and N. J. Navimipour, “An improved genetic algorithm for task scheduling in the cloud environments using the priority queues: Formal verification, simulation, and statistical testing,” *Journal of Systems and Software*, vol. 124, pp. 1–21, 2017.
- [14] J. Li, R. Zhang, and Y. Yang, “Multi-auv autonomous task planning based on the scroll time domain quantum bee colony optimization algorithm in uncertain environment,” *PloS one*, vol. 12, no. 11, p. e0188291, 2017.
- [15] H. Wu and R. Xiao, “Flexible wolf pack algorithm for dynamic multidimensional knapsack problems,” *Research*, 2020.
- [16] M. Yan, H. Yuan, J. Xu, Y. Yu, and L. Jin, “Task allocation and route planning of multiple uavs in a marine environment based on an improved particle swarm optimization algorithm,” *EURASIP Journal on Advances in Signal Processing*, pp. 1–23, 2021.
- [17] S. Biswas, S. G. Anavatti, and M. A. Garratt, “Particle swarm optimization based co-operative task assignment and path planning for multi-agent system,” in *2017 IEEE Symposium Series on Computational Intelligence (SSCI)*, 2017, pp. 1–6.
- [18] A. M. Wells, N. T. Dantam, A. Shrivastava, and L. E. Kavraki, “Learning feasibility for task and motion planning in tabletop environments,” *IEEE Robotics and Automation Letters*, vol. 4, no. 2, pp. 1255–1262, 2019.
- [19] S. Omidshafiei, J. Pazis, C. Amato, J. P. How, and J. Vian, “Deep decentralized multi-task multi-agent reinforcement learning under partial observability,” in *Proceedings of the 34th International Conference on Machine Learning*, vol. 70, 06–11 Aug 2017, pp. 2681–2690.
- [20] M. Liu, H. Ma, J. Li, and S. Koenig, “Task and path planning for multi-agent pickup and delivery,” in *Proceedings of the International Joint Conference on Autonomous Agents and Multiagent Systems (AAMAS)*, 2019.
- [21] H. Zhang, W. Du, J. Shan, Q. Zhou, Y. Du, J. B. Tenenbaum, T. Shu, and C. Gan, “Building cooperative embodied agents modularly with large language models,” *arXiv preprint arXiv:2307.02485*, 2023.
- [22] J. Ruan, Y. Chen, B. Zhang, Z. Xu, T. Bao, G. Du, S. Shi, H. Mao, X. Zeng, and R. Zhao, “Tptu: Task planning and tool usage of large language model-based ai agents,” *arXiv preprint arXiv:2308.03427*, 2023.
- [23] C. Baier and J.-P. Katoen, *Principles of Model Checking*. MIT press, 2008.
- [24] R. Koymans, “Specifying real-time properties with metric temporal logic,” *Real-Time Systems*, vol. 2, no. 4, pp. 255–299, 1990.
- [25] O. Maler and D. Nickovic, “Monitoring temporal properties of continuous signals,” in *International Symposium on Formal Techniques in Real-Time and Fault-Tolerant Systems*. Springer, 2004, pp. 152–166.
- [26] X. Luo, Y. Kantaros, and M. M. Zavlanos, “An abstraction-free method for multirobot temporal logic optimal control synthesis,” *IEEE Transactions on Robotics*, 2021.
- [27] M. Guo and D. V. Dimarogonas, “Task and motion coordination for heterogeneous multiagent systems with loosely coupled local tasks,” *IEEE Transactions on Automation Science and Engineering*, vol. 14, no. 2, pp. 797–808, 2016.
- [28] X. Luo and M. M. Zavlanos, “Temporal logic task allocation in heterogeneous multi-robot systems,” *IEEE Transactions on Robotics*, vol. 38, no. 6, pp. 3602–3621, 2022.
- [29] Y. E. Sahin, P. Nilsson, and N. Ozay, “Multirobot coordination with counting temporal logics,” *IEEE Transactions on Robotics*, vol. 36, no. 4, pp. 1189–1206, 2019.
- [30] A. M. Jones, K. Leahy, C. Vasile, S. Sadraddini, Z. Serlin, R. Tron, and C. Belta, “Scratches: Scalable and robust algorithms for task-based coordination from high-level specifications,” in *Proc. Int. Symp. Robot. Res.*, 2019, pp. 1–16.
- [31] P. Schillinger, M. Bürger, and D. V. Dimarogonas, “Decomposition of finite ltl specifications for efficient multi-agent planning,” in *International Symposium on Distributed Autonomous Robotic Systems*, 2016.
- [32] P. Schillinger, M. Bürger, and D. V. Dimarogonas, “Simultaneous task allocation and planning for temporal logic goals in heterogeneous multi-robot systems,” *The International Journal of Robotics Research*, vol. 37, no. 7, pp. 818–838, 2018.
- [33] Y. Kantaros and M. M. Zavlanos, “Stylus*: A temporal logic optimal control synthesis algorithm for large-scale multi-robot systems,” *The International Journal of Robotics Research*, vol. 39, no. 7, pp. 812–836, 2020.
- [34] X. Yu, X. Yin, S. Li, and Z. Li, “Security-preserving multi-agent coordination for complex temporal logic tasks,” *Control Engineering Practice*, vol. 123, p. 105130, 2022.
- [35] L. Li, Z. Chen, H. Wang, and Z. Kan, “Fast task allocation of heterogeneous robots with temporal logic and inter-task constraints,” *IEEE Robotics and Automation Letters*, 2023.
- [36] J. Bonnet, M.-P. Gleizes, E. Kaddoum, S. Rainjonneau, and G. Flandin, “Multi-satellite mission planning using a self-adaptive multi-agent system,” in *2015 IEEE 9th International Conference on Self-Adaptive and Self-Organizing Systems*, 2015, pp. 11–20.
- [37] Q. Yang, Z. Luo, W. Song, and R. Parasuraman, “Self-reactive planning of multi-robots with dynamic task assignments,” in *2019 International Symposium on Multi-Robot and Multi-Agent Systems (MRS)*, 2019, pp. 89–91.
- [38] M. Faroni, A. Umbrico, M. Beschi, A. Orlandini, A. Cesta, and N. Pedrocchi, “Optimal task and motion planning and execution for multiagent systems in dynamic environments,” *IEEE Transactions on Cybernetics*, pp. 1–12, 2023.
- [39] S. Choudhury, J. K. Gupta, M. J. Kochenderfer, D. Sadigh, and J. Bohg, “Dynamic multi-robot task allocation under uncertainty and temporal constraints,” *Autonomous Robots*, vol. 46, no. 1, pp. 231–247, 2022.
- [40] D. Tian, H. Fang, Q. Yang, Z. Guo, J. Cui, W. Liang, and Y. Wu, “Two-phase motion planning under signal temporal logic specifications in partially unknown environments,” *IEEE Transactions on Industrial Electronics*, vol. 70, no. 7, pp. 7113–7121, 2023.
- [41] M. Ben-Ari, “A primer on model checking,” *ACM Inroads*, vol. 1, no. 1, pp. 40–47, 2010.

- [42] P. Gastin and D. Oddoux, "Fast LTL to Büchi automata translation," in *Proceedings of the 13th International Conference on Computer Aided Verification*, 2002, pp. 53–65.
- [43] X. Ding, S. L. Smith, C. Belta, and D. Rus, "Optimal control of markov decision processes with linear temporal logic constraints," *IEEE Transactions on Automatic Control*, vol. 59, no. 5, pp. 1244–1257, 2014.
- [44] M. Kloetzer and C. Mahulea, "Accomplish multi-robot tasks via petri net models," in *2015 IEEE International Conference on Automation Science and Engineering (CASE)*, 2015, pp. 304–309.
- [45] K. Leahy, Z. Serlin, C.-I. Vasile, A. Schoer, A. M. Jones, R. Tron, and C. Belta, "Scalable and robust algorithms for task-based coordination from high-level specifications (scratches)," *IEEE Transactions on Robotics*, vol. 38, no. 4, pp. 2516–2535, 2022.
- [46] P. Schillinger, M. Bürger, and D. V. Dimarogonas, "Hierarchical ltl-task mdps for multi-agent coordination through auctioning and learning," *The International Journal of Robotics Research*, 2019.
- [47] Y. Kantaros and M. M. Zavlanos, "Sampling-based optimal control synthesis for multirobot systems under global temporal tasks," *IEEE Transactions on Automatic Control*, vol. 64, no. 5, pp. 1916–1931, 2018.
- [48] N. Piterman, A. Pnueli, and Y. Sa'ar, "Synthesis of reactive(1) designs," in *Verification, Model Checking, and Abstract Interpretation*, 2006, pp. 364–380.
- [49] V. Vasilopoulos, Y. Kantaros, G. J. Pappas, and D. E. Koditschek, "Reactive planning for mobile manipulation tasks in unexplored semantic environments," in *International Conference on Robotics and Automation*, 2021.
- [50] C. K. Verginis and D. V. Dimarogonas, "Multi-agent motion planning and object transportation under high level goals," in *IFAC World Congress*, 2018.
- [51] B. Lacerda, D. Parker, and N. Hawes, "Optimal and dynamic planning for markov decision processes with co-safe ltl specifications," in *2014 IEEE/RSJ International Conference on Intelligent Robots and Systems*, 2014, pp. 1511–1516.
- [52] S. Feyzabadi and S. Carpin, "Multi-objective planning with multiple high level task specifications," in *2016 IEEE International Conference on Robotics and Automation (ICRA)*, 2016, pp. 5483–5490.
- [53] C. Belta, B. Yordanov, and E. A. Gol, *Formal Methods for Discrete-time Dynamical Systems*. Springer, 2017, vol. 15.
- [54] Z. Liu, M. Guo, and Z. Li, "Time minimization and online synchronization for multi-agent systems under collaborative temporal logic tasks," *Automatica*, vol. 159, p. 111377, 2024.
- [55] Smith, "The contract net protocol: High-level communication and control in a distributed problem solver," *IEEE Transactions on Computers*, vol. C-29, no. 12, pp. 1104–1113, 1980.
- [56] F. Faruq, D. Parker, B. Laccrda, and N. Hawes, "Simultaneous task allocation and planning under uncertainty," in *2018 IEEE/RSJ International Conference on Intelligent Robots and Systems (IROS)*. IEEE, 2018, pp. 3559–3564.
- [57] C. K. Verginis and D. V. Dimarogonas, "Multi-agent motion planning and object transportation under high level goals," *IFAC-PapersOnLine*, vol. 50, no. 1, pp. 15 816–15 821, 2017.
- [58] D. C. Kozen and D. C. Kozen, "Depth-first and breadth-first search," *The Design and Analysis of Algorithms*, pp. 19–24, 1992.

SUPPLEMENTARY MATERIALS

Movie s1. Simulation and Experiment of dynamic tasks in a hospital environment.

Table sI. Definitions of agents, behaviors, objects and interested regions.

Table sII. sc-LTL formulas of simulation.

Table sIII. sc-LTL formulas of experiment.

TABLE I
DEFINITIONS OF AGENTS, BEHAVIORS, OBJECTS AND INTERESTED REGIONS

Agent	Ability	Label
Junior Doctor	assist operation, transfer, medicine, record, disinfect, clean	<i>JD</i>
Senior Doctor	preside operation, disinfect, medicine	<i>SD</i>
Nurse	transfer, clean, supply, record	<i>Nu</i>
Interactive Object	Description	Label
Family Visitor	A family member visiting the patient	<i>FV</i>
Vomiting Patient	A patient who suddenly vomited and contaminated the current region	<i>VP</i>
Senior patient	A patient with a mild illness	<i>SP</i>
Junior Patient	A patient with a serious illness	<i>JP</i>
Cooperative Behavior	Ability and Object Requirement	Label
primary operate	assist operation: 1, supply: 2, senior patient: 1	<i>P</i>
advance operate	assist operation: 2, preside operation: 1, supply: 2, junior patient: 1	<i>A</i>
disinfect ground	clean: 1	<i>D</i>
transfer patient	transfer: 2, junior or vomiting patient: 1	<i>T</i>
collect information	record : 1	<i>C</i>
guide visitor	transfer: 1, family visitor or senior patient: 1	<i>G</i>
supply medicine	medicine: 1, record: 1	<i>M</i>
radiate	clean: 1, disinfect: 1	<i>R</i>

TABLE II
SC-LTL FORMULAS FOR SIMULATION

Offline Formula	Description
φ_{b1}	$\Diamond(T_{w1,o1}^1 \wedge \neg P_{o1,o1}^1 \wedge \Diamond(P_{o1,o1}^1 \wedge \neg R_{o1,o1}^\emptyset \wedge \Diamond T_{o1,w1}^1 \wedge \Diamond R_{o1,o1}^\emptyset))$: Eventually transport the patient 1 from $w1$ to $o1$ and perform a primary operation for him. Then, transport him back and radiate to the operation $o1$.
φ_{b2}	$\Diamond(C_{w3,w3}^\emptyset \wedge \Diamond(T_{w3,o4}^2 \wedge \Diamond A_{o4,o4}^2 \wedge \neg R_{o4,o4}^\emptyset \wedge \Diamond(T_{o4,w3}^2 \wedge \neg A_{o4,o4}^2 \wedge \Diamond C_{w3,w3}^\emptyset) \wedge \Diamond(R_{o4,o4}^\emptyset \wedge \Diamond D_{o4,o4}^\emptyset)))$: Record the situation of inpatient ward $w3$ first. Then transport patient 2 from $w3$ to operation $o4$ and perform an advanced operation for this patient at $o4$. After that, transport the patient back to $w3$ and Record the situation; radiate and disinfect the ground of $o4$.
φ_{b3}	$\Diamond(C_{w3,w3}^\emptyset \wedge \neg T_{w3,e2}^3 \wedge \Diamond D_{w3,w3}^\emptyset \wedge \Diamond T_{w3,e2}^3)$: Record the situation of ward $w3$ and transport the patient 3 into the exit $e2$ and disinfect the ground of $w3$.
φ_{b4}	$\Diamond D_{w7,w7}^\emptyset \wedge \Diamond(C_{w7,w7}^\emptyset \wedge \neg M_{w7,w7}^\emptyset \wedge \Diamond M_{w7,w7}^\emptyset)$: Disinfect the ground of ward $w7$, record the information and supply the medicines at $w7$.
φ_{b5}	$\Diamond(C_{w7,w7}^\emptyset \wedge \neg G_{w7,e3}^4 \wedge \Diamond G_{w7,e3}^4) \wedge \neg D_{w7,w7}^\emptyset \cup C_{w7,w7}^\emptyset$: Collect information in ward $w7$ then guide the patient 4 from ward $w7$ to exit $e3$. Do not disinfect the ground of $w7$ before collecting the information.
φ_{b6}	$\Diamond(T_{h5,w5}^5 \wedge \Diamond C_{w5,w5}^\emptyset \wedge \Diamond M_{w5,w5}^\emptyset) \wedge \neg M_{w5,w5}^\emptyset \cup C_{w5,w5}^\emptyset$: Transport patient 5 form hall $h5$ to $w5$ and supply medicine and collect information of $w5$. Do not supply medicine before collect the information.
Online Formula	Description
φ_{VP}	$\Diamond(T_{i,i}^u \wedge \Diamond R_{i,i}^\emptyset \wedge \Diamond D_{i,j}^\emptyset) \wedge \neg Nu_i \cup R_{i,i}^\emptyset$: When a patient has vomited in region i , transport him to region j , radiate and disinfect region i . Nurses should not enter region i before radiate.
φ_{JP}	$\Diamond G_{i,j}^u \wedge \Diamond R_{i,i}^\emptyset \wedge \neg JD_i \cup R_{i,i}^\emptyset$: When a junior patient comes to region i , guide him to region j and radiate the region i , the junior doctor should not enter i until radiate.
φ_{SP}	$\Diamond(T_{i,j}^u \wedge (\bigwedge_{\ell=1 \dots 3} \neg SP_{o_\ell}) \wedge \Diamond M_{j,j}^\emptyset \wedge \Diamond C_{j,j}^\emptyset)$: When a senior patient comes to region i , transport him to region j and do not enter operation rooms $o1, o2, o3$; then supply medicine and collect information.
φ_{FV}	$\Diamond G_{i,j}^u \wedge (\bigwedge_{\ell=1 \dots 5} \neg FV_{o_\ell})$: When a family visitor comes, guide him to his goal and do not enter the operation rooms $o1, \dots, o5$.

TABLE III
SC-LTL FORMULAS FOR EXPERIMENT

Formula	Description
φ_{b_1}	$\Diamond(C_{w3,w3}^{\emptyset} \wedge \Diamond(T_{w3,o4}^1 \wedge \Diamond(A_{o4,o4}^1 \wedge \neg R_{o4,o4}^1 \wedge \Diamond(T_{o4,w3}^1 \wedge \neg A_{o4,o4}^1 \wedge \Diamond C_{w3,w3}^{\emptyset})) \wedge \Diamond R_{o4,o4}^{\emptyset}))$: Collect information in $w3$, transport the patient 1 from $w3$ to $o4$ and perform an advanced operation for him. Then, transport him back and collect the information; radiate $o4$.
φ_{b_2}	$\Diamond(C_{w3,w3}^{\emptyset} \wedge \neg T_{w3,e2}^2 \wedge \Diamond D_{w3,w3}^{\emptyset} \wedge \Diamond T_{w3,e2}^2)$: Collect information in $w3$, transport the patient 2 from $w3$ to $e2$ and disinfect the area $w3$.
φ_{b_3}	$\Diamond(T_{h5,w2}^3 \wedge \Diamond C_{w2,w2}^{\emptyset} \wedge \Diamond M_{w2,w2}^{\emptyset})$: Transport patient 3 from $h5$ to $w2$ then collect the information in $w2$, and supply medicine at $w2$.
φ_{b_4}	$\neg M_{w2,w2}^{\emptyset} \cup C_{w2,w2}^{\emptyset}$: Do not supply medicine at $w2$ before collecting information.
φ_{VP}	$\Diamond(T_{i,i}^u \wedge \Diamond R_{j,j}^{\emptyset} \wedge \Diamond D_{i,j}^{\emptyset}) \wedge \neg Nu_i \cup R_{i,i}^{\emptyset}$: When a patient has vomited in region i , transport him to region j , radiate and disinfect region i . Nurses should not enter region i beforehand.
φ_{JP}	$\Diamond G_{i,j}^u \wedge \Diamond R_{i,i}^{\emptyset} \wedge \neg JD_i \cup R_{i,i}^{\emptyset}$: When a junior patient comes to region i , guide him to region j and radiate the region i , the junior doctor should not enter i beforehand.
φ_{SP}	$\Diamond(T_{i,j}^u \wedge (\bigwedge_{\ell=1..3} \neg SP_{o_\ell}) \wedge \Diamond M_{j,j}^{\emptyset} \wedge \Diamond C_{j,j}^{\emptyset})$: When a senior patient comes to region i , transport him into region j and do not enter operation rooms $o1, o2, o3$; then supply medicine and collect information.
φ_{FV}	$\Diamond G_{i,j}^u \wedge (\bigwedge_{\ell=1..5} \neg FV_{o_\ell})$: When a family visitor comes, guide him to his goal and do not enter the operation rooms $o1, \dots, o5$.